MONASH University

Saline-water Upconing in Heterogeneous Aquifers

Maozhu Tang

Bachelor of Engineering (Honors)

A thesis submitted for the degree of Master of Engineering Science

(Research) at Monash University in (2017)

Faculty of Engineering

April, 2017

Copyright Notice

Abstract

The existence of fresh groundwater overlying saltwater in groundwater system is ubiquitous in many inland aquifers as well as in most coastal aquifers. The utilization of freshwater resources in those areas is therefore highly constrained by the presence of saline-water upconing, a physical process that occurs when salty groundwater rises towards a pumping well. This research investigated this process in heterogeneous aquifers by using models in ideal scenarios. Specifically, two scenarios were included: (I) pumping with an aquitard below the well, and (II) pumping in a randomly heterogeneous aquifer. An axisymmetric geometry with the two different settings was implemented in the numerical code SEAWAT, which solves coupled density-dependent flow and solute transport equations. After a certain pumping time, the extracted water will be salinized to a certain degree (i.e. 2%), thus forcing the well's shut-off; the period before reaching 2% is defined as the available pumping duration of the effect of aquifer heterogeneity on saline-water upconing, and was used as a key indicator.

Available pumping durations from numerical simulations for two heterogeneous settings are compared with that of a homogeneous case. For each heterogeneous setting, there were two main findings. In the case of pumping above an aquitard, linear relations between pumping durations and hydraulic conductivities were established for varied dimensions of aquitards, and there was a critical location of an aquitard where the well showed the highest pumping efficiency. For pumping occurring in a randomly heterogeneous aquifer, it was found that increasing degrees of heterogeneity in aquifers might improve the pumping efficiency. Also, hydraulic conductivities in two directions showed different patterns of impact on the pumping efficiency. The horizontal hydraulic conductivity was inversely related to the final pumping duration, while the vertical one was positively correlated to the early stage of pumping when only freshwater was pumped out.

Declaration

This thesis contains no material which has been accepted for the award of any other degree or diploma at any university or equivalent institution and that, to the best of my knowledge and belief, this thesis contains no material previously published or written by another person, except where due reference is made in the text of the thesis.

Signature: 

Print Name: Maozhu Tang

Date: April, 2017

Acknowledgement

Firstly, I would like to thank my main supervisor Dr. Edoardo Daly for his patience and guidance. When my previous main supervisor Dr. Chunhui Lu resigned from Monash University at the mid of my candidature, he encouraged and guided me for continuing the research study. He is so patient that every time he will make detailed comments on my writings, and sometimes drops in my office to see how my research is going. I also want to show sincere thanks to my associate-supervisor Dr. Chunhui Lu. When he was in Monash, he gave me a lot of guidance on research studies, and he also provided me a chance to experience research life in Hohai University, where it leads researches regarding to groundwater in China.

I also would like to say thanks to Mrs. Jenny Manson from Departmental of Civil Engineering, who is always here to help; thank my friends in the office; thank my parents for consistent support to let me continue the academic study; thank my boyfriend who is always standing by my side, supporting and encouraging me. Last but not the least, I would like to thank Faculty of Engineering to provide scholarship of Monash Graduate Scholarship (MGS) to support my two-year research study.

This work is dedicated to my University, and hoping that she can excels in researches in future.

Maozhu Tang

April, 2017

Table of Contents

List of Figures

Figure **Page**

List of Tables

Table **Page**

Chapter 1

INTRODUCTION

Groundwater is water stored in pores of soil particles and rock fractures underneath the Earth's surface, and it represents a major source of freshwater on Earth. Groundwater dynamics occur at different length and time scales (from hours to millennia) as a result of recharging from and discharging to surface water bodies. Using groundwater as a source of freshwater shows several advantages compared with surface water: (I) groundwater serves as an accessible freshwater source during dry seasons or in some dry regions around the world, (II) it is less vulnerable to pollutions, and (III) the amount of groundwater stored is larger than that of surface water. Groundwater is widely seen in agricultural, municipal, and industrial uses, and the demand for it is increasing. For example, groundwater stored in coastal aquifers, where nearly half of the global population is located, is considered a vital freshwater resource and its demand is increasing since population densities in these regions are growing due to economic development.

As the major freshwater resource, groundwater quality needs to be ensured. For example, for human consumptions, a high level of quality should be achieved. Listed in the report of Groundwater Quality in Australia [1], the following sources can be a threat to the groundwater quality for usage:

- Salinity
- Acidity
- Nutrients
- Contaminants such as heavy metals, industrial chemicals and pesticides.

Although groundwater flowing through rocks and subsurface soils can cause some levels of substances dissolved in it, the ground itself has a certain ability to filter out these matters. However, excessive human activities have put too much pressure on exiting groundwater resources so that they are suffering degradation around the world.

1.1 Salinity intrusion process

The threat caused by salinity to groundwater quality draws much attention, because in coastal aquifers, the adjacent seawater can cause salinity intrusion into the fresh groundwater zone that stores the major water resource in these regions. For example, the world-widely occurring Seawater Intrusion (SWI) issue has been recognized as a major threat to coastal aquifers, posing challenges to coastal groundwater management in many countries such as Australia and US. Under undisturbed conditions, the seaward movement of excessive freshwater (i.e. recharge minus discharge) is balanced with the steady-state seawater below. Activities that break this equilibrium (e.g. sea-level rise or excessive groundwater pumping) will lead to the landward movement of seawater until a new balance is reached. Figure 1.1 shows a representative vertical cross-section of a coastal aquifer with SWI, presented in [2]. The interaction between fresh groundwater and intruded saline seawater leads to the mixing of them (i.e. “transition zone” shown in the figure), and this mixing zone is with varied concentrations and densities. The mixing zone is considered as the main indicator of intrusion extent. “Interface” shown in the figure is considered as a simplified indicator of the transition zone.

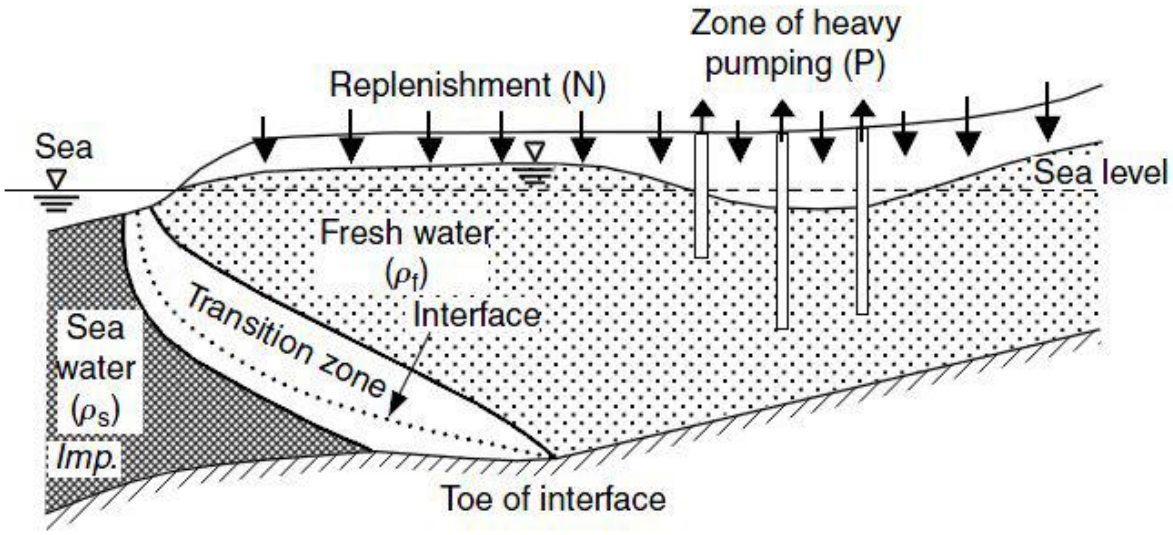

Figure 1.1. A typical cross sections of seawater intrusion in coastal aquifers (Phreatic aquifer) with recharge and pumping. Not drawn to scale. [2]

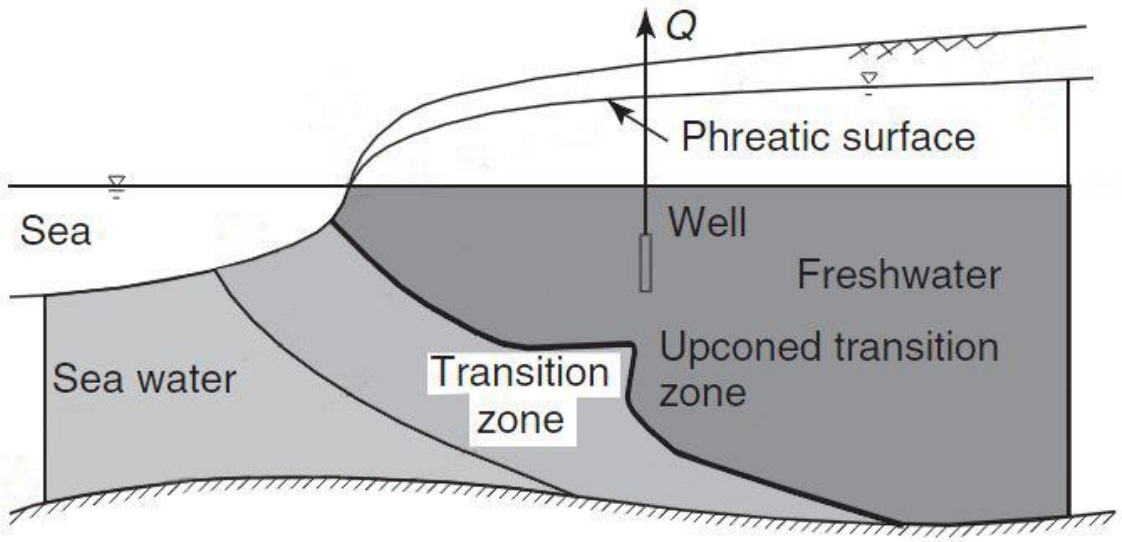

Figure 1.2. The upconing process in a simplified vertical cross section of a coastal aquifer. Not drawn to scale. [3]

When a partially penetrating well is located in an aquifer with SWI occurring, the extraction of freshwater will result in a vertical hydraulic gradient, thus causing a local upward movement of seawater into the upper freshwater zone, forming a shape of cone. This physical process of saline groundwater rising into the upper freshwater zone is called Saline-water Upconing (SU). SU is another process causing the salinity intrusion into freshwater. A simplified cross-section of SU at the regional scale is shown in Figure 1.2 [3]. Besides SU in coastal aquifers, it is also a ubiquitous process in some inland aquifers, where freshwater and saline-water are stratified. Saline-water occurring in inland aquifers may be a results of dissolution of sediments or rocks. Overall, SU is another intrusion process of saline-water, which may directly result in the pumping of salinized water.

1.2 Salinity intrusion examples

Salinity encroachment has been observed in many areas and especially coastal regions from the late 20^{th} century. For example, in the coast of Laizhou Bay, Shandong Province of China, available data showed that SWI was firstly observed in that region from 1971 [4], when the zones of influence were just some small and isolated areas. Gradually, with the increase of human activities, these areas spread out and connected to larger regions. Specifically, in 1979 the area of SWI was just 16 km^2 but 10 years later it increased to nearly 238 km^2. However, in 1990 when the precipitation doubly increased, the continuously increased rate of rise of influenced areas was slowed by the high recharge rate.

There are also some field observations available for upward salinity intrusion. For example, Figure 1.3 shows the salinity profile of an observation well before and after pumping from a study

of SWI in South East of South Australia [5]. The rise of salinized water (especially salinity larger than 10000 uS cm^{-1}) after pumping (yellow curve) suggests the upward movement of salts in that aquifer due to pumping.

Saline-water intrusion is a harmful process because the salinization of aquifers, soils or surface water can negatively impact the environmental and economic development. It is estimated that nearly 2527 ha of agriculture may be suffering from SWI in South Australia [5].

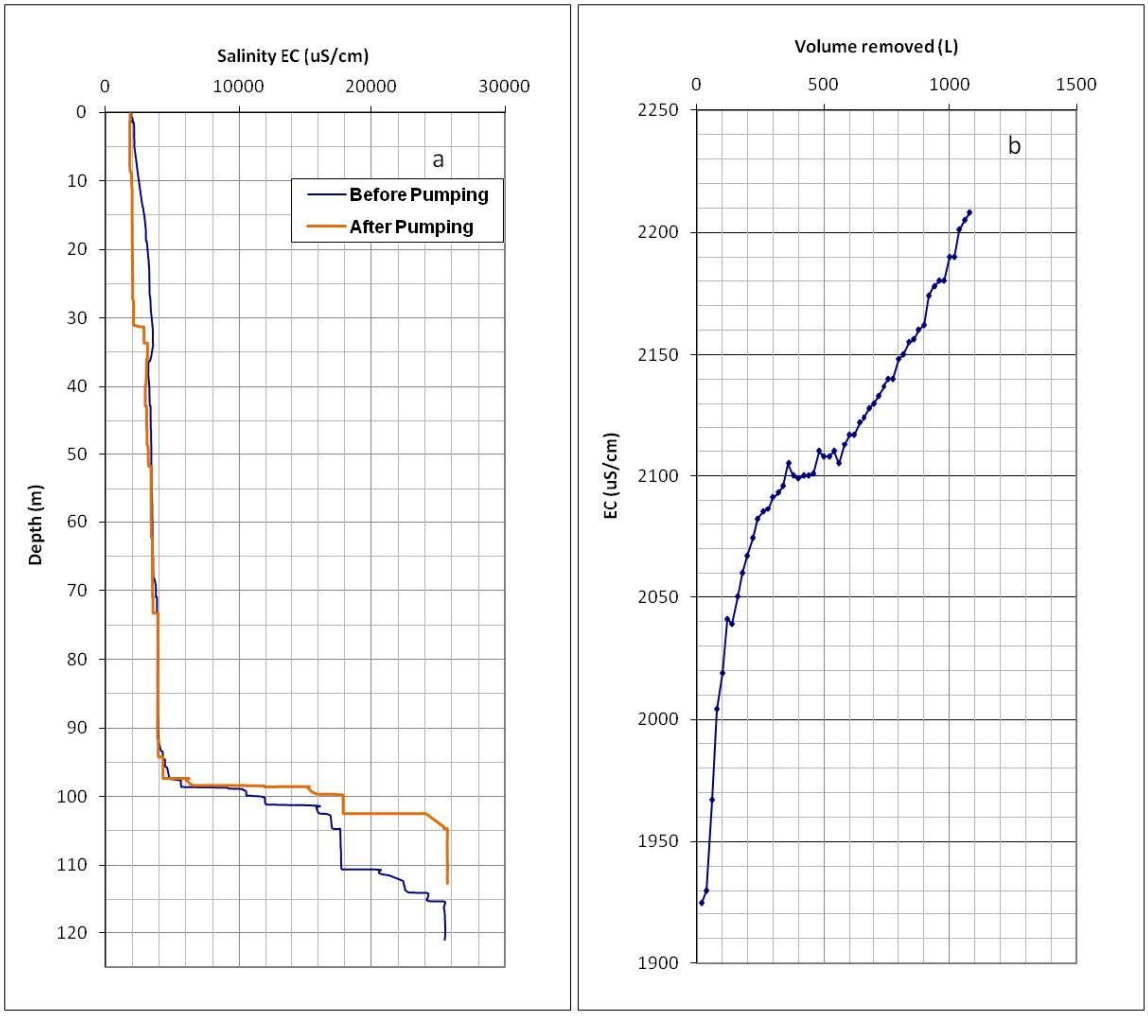

Figure 1.3. Observation well salinity profile in the report [5]: before and after pumping (left); volume pumped versus water salinity (right)

1.3 Proposed research

The growing trend of deteriorating water quality and aquifers urges the related professionals to better understand the mechanisms of SU, and thus to improve the sustainable management of groundwater resources. Therefore, this thesis aims to improve the scientific understanding of the SU process. More specifically, the focus is on the SU process in geologically heterogeneous aquifers, since heterogeneity has not been largely explored in previous studies. Two specific aims are (I) examining the efficiency of a pumping well under threats of SU when a low-permeability horizontal layer is located in the aquifer, and (II) understanding of pumping efficiency of an extraction well under threats of SU in an aquifer with random distributions of hydraulic conductivity (K). This research is mainly motivated by the work in [6, 7] for the following reasons:

1. Heterogeneity in hydraulic conductivity is an inherent property of an aquifer. When considering transport of dissolved solutes, the heterogeneity is highly associated with the hydrodynamic dispersion, which is the controlling process of SU. So it is hypothesized that heterogeneity in geological formations will show a great impact on the upconing efficiency.
2. The scale of heterogeneity is a vital factor in terms of the mixing zone thickness in SWI process. Upconing can be regarded as a vertical SWI, so that the large scale heterogeneity (i.e. stratified aquifer) and small-scale heterogeneity (i.e. random distribution of K fields) are hypothesized to show different impacts on SU.

The research project was based on modelling. Simulations of an idealized aquifer were used to test the effect of aquifer heterogeneity on SU. The software SEAWAT used in this research has been used and modified by many researches (refer to Table 2.1). The primary variable of interest in this research is the available pumping duration, defined as the duration from the

beginning of pumping to the time when the relative salinity of pumped water reaches 2%, which has been adopted in published studies [e.g., 8, 9].

1.4 Outline of thesis

The thesis includes 5 chapters. A brief introduction is provided in this Chapter. A comprehensive literature review is provided in Chapter 2. The SU process in an aquifer with a low-permeability horizontal layer is shown in Chapter 3. The SU process in an aquifer with random distributions of K fields is presented in Chapter 4. Chapter 5 summarizes the conclusions and implications of the research results and also discusses the limitations of the current study.

Chapter 2

LITERATURE REVIEW

This literature review mainly focuses on studies concerning SU. Although the more general SWI has been investigated in many studies, and there are comprehensive literature reviews published [e.g., 6, 10, 11], a smaller amount of works focused specifically on SU is available. The study of SU has been carried out mainly using mathematical models, with limited laboratory experiments and field investigations. This literature review summarized the published methods to study SU, which were categorized into mathematical models, laboratory scale physical models, and field investigation.

2.1 Mathematical models

Mathematical models serve as an efficient tool for predictions of groundwater-flow and solute transport behaviors in aquifers. The denser saltwater underlying freshwater represents the standard scenario for mathematical models for the SU problem. These two fluids with varied densities are miscible, so that in a real situation, a transition zone with varied concentrations and densities occurs between them. The solution of such a SU model requires the simultaneous solutions of the fluid low equation and solute transport equation. Reilly and Goodman [12] provided a detailed description of governing equations for SU models. When pumping begins, the hydrodynamic dispersion may cause the transition zone to further develop, and the difficulty here is to predict the behavior of the transition zone for this highly coupled and non-linear system. Generally the two mathematical models used are sharp-interface and variable-density flow models.

The sharp interface model assumes that freshwater and saline water are immiscible, so that the transition zone is replaced by an abrupt interface. Although this model significantly simplifies the SU problem, in situations where the transition zone is very thin compared with the thickness of the aquifer, it works as a good indicator of SU. At the early stage of SU studies, when computing capabilities were not very advanced, sharp interface models were widely used to approximate SU.

A variable-density flow model better describes the SU process, because it includes the realistic mixing between freshwater and saline-water. At present, variable-density flow models are favorable to understand and predict SU.

2.1.1 Sharp interface model

In a sharp interface model, rise of the assumed abrupt interface between freshwater and saline water represents the upconing process. Figure 2.1 shows a typical schematic of the physics of SU in a sharp interface model in [12]. The pumping will lead to the pressure reduction in the upper freshwater zone, and thus the interface will move upward until a new equilibrium is achieved, forming a stable upward cone. The increase of the pumping rate will further rise the interface. However, if the pumping rate is so high that, before reaching a balance, the interface intercepts the well bottom, an unsteady upconing occurs, leading to the salinity of pumped water. Such a critical condition is associated with a critical value for the pumping rate of the well, usually called critical pumping rate or maximum permissible rate in the literature. This physics was firstly introduced by Muskat and Wycokoff [13] based on the oil-water scenario, and is also widely applied in a sharp interface model of SU study.

For sustainable groundwater usage, the critical pumping rate needs to be avoided. Applying a sharp interface model as a first approximation of critical conditions for SU is a research topic of great interest. This is usually achieved through analytic solutions or semi-analytic solutions. The

parameters representing critical conditions mainly include the critical pumping rate, and its associated critical interface-rise ratio. The latter one is a widely used dimensionless parameter for many researches [e.g., 14, 15-19], and is defined as the ratio of distance between interface and bottom of well to the aquifer thickness.

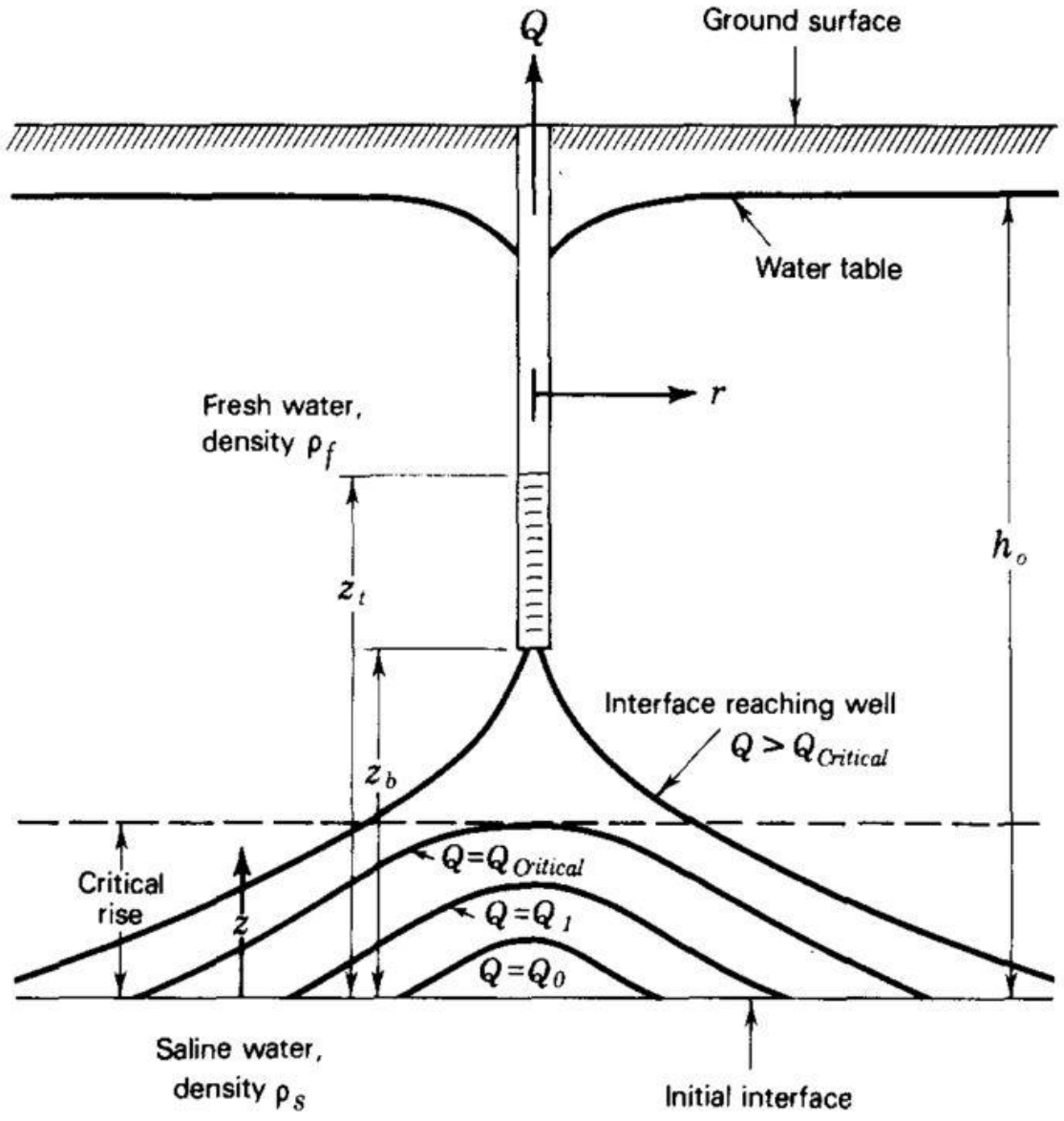

Figure 2.1. Indication of the physical process of SU in a sharp interface model [12]

Fully solving a sharp interface model still needs to simultaneously solve the flow of saline water and flow of freshwater, which should satisfy specified initial and boundary conditions. However, the boundary condition at the sharp interface is highly non-linear and is not known initially; this poses the difficulty to get exact solutions. This interface flow problem is often further simplified with the Ghyben-Herzberg solution [11] based on the assumptions of static seawater and vertical potential lines in freshwater region (i.e. Dupuit assumption in freshwater region). The Ghyben-Herzberg solution was the first formulation for saline-water intrusion problem, which expressed the relation between the distance from sea-level to phreatic surface and to the interface, as shown in Figure 2.2 and expressed as,

$$z = \frac{\rho_f}{\rho_s - \rho_f} h_f, \tag{2.1}$$

where z is the distance from sea-level to the interface, h_f is the distance from sea-level to the phreatic surface, ρ_s is the saltwater density, and ρ_f is the freshwater density. This ratio $\frac{\rho_f}{\rho_s - \rho_f}$ is a constant under certain conditions (for example, at 20 ^{o}C, ρ_f and ρ_s are 1000 and 1025 kg m^{-3} respectively, which results in the ratio equaling 40 [20]); therefore it suggests that every meter of drawdown in phreatic surface results in 40 meters rise of the interface.

Generally, the published studies adopting Ghyben-Herzberg solution can be divided into two categories: confined or unconfined interface flow, that is upconing in local scale [e.g., 18, 19] and combinations of confined (or unconfined) interface flow with confined (or unconfined) flow, that is upconing in coastal aquifers [e.g., 21]. For the first category, more recent studies include Garabedian [22] and Hendizadeh et al. [23]. Both of them utilized the method that was firstly conceptualized in the work by Muskat [24], as indicated in Figure 2.3 for pressure distributions in two fluids, to determine the value of critical interface rise. Curve 1 and curve 2 represent freshwater

and saltwater pressure distributions respectively before pumping. At this initial state, above the interface, freshwater pressure is larger than that of saltwater, but their difference becomes smaller from the top to the interface. When pumping is introduced, the curve 2 is stable, but the freshwater pressure decreases immediately. Increasing the pumping rate will further reduce the freshwater pressure, which is indicated by the movement from curve 3 to curve 5. Curve 5 represents the unstable state of interface, meaning that saltwater intercepts the bottom of well. So the point C represents the critical condition. The equality of both pressures of two fluids and their pressure gradients at point C contributes to determining the critical interface rise. According to this method, Garabedian [22] solved the critical interface rise for an aquifer with a partially penetrating well, no-flow conditions at the top and bottom, and a constant head conditions at a known radial distance. They compared the analytic results with numerical ones from SEAWAT, and they observed obvious numerical dispersion, leading to a variance of results around the well. They also concluded that freshwater zone thinning effect due to interface rise could not be ignored through the comparison with numerical results from Reilly and Goodman [12], otherwise, the prediction of critical condition could be overestimated. Hendizadeh et al. [23] determined critical conditions for aquifers with finite horizontal well and finite vertical well. They concluded that total critical pumping rate increased in both longer vertical and horizontal wells, but linearly decreased with their depth. The most well-known study using Ghyben-Herzberg solution in regional coastal aquifer is that of Strack [21], who used a single potential (Strack's potential) to solve the interface flow extension in a coastal aquifer. Applying such a potential was advantageous when the position and geometry of the interface were unknown, thus the boundary condition is unknown. Application of that potential in their research was to calculate the critical pumping rate for a fully penetrating well in a Strack's coastal region.

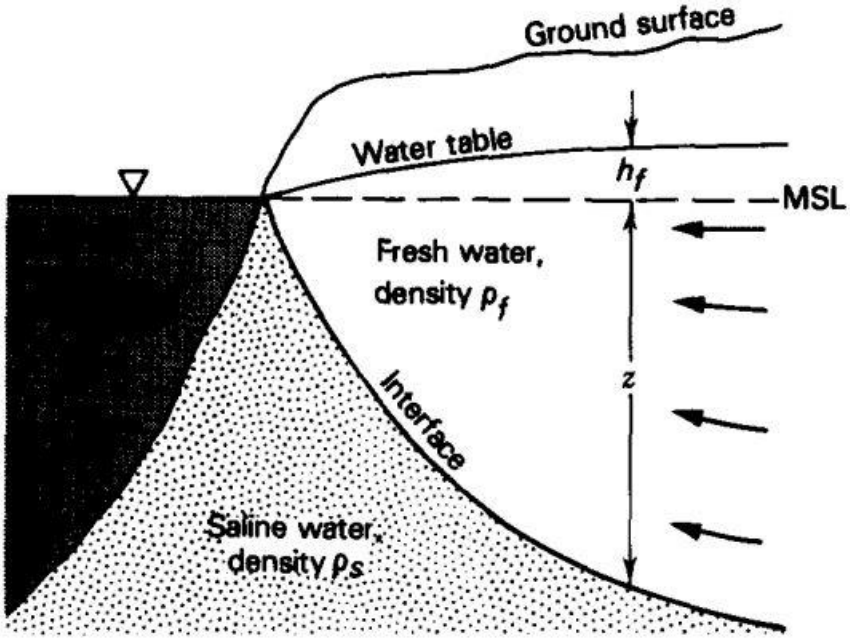

Figure 2.2. The Ghyben-Herzberg principle in a cross-section of a coastal aquifer [11]. MSL stands for Mean Sea Level.

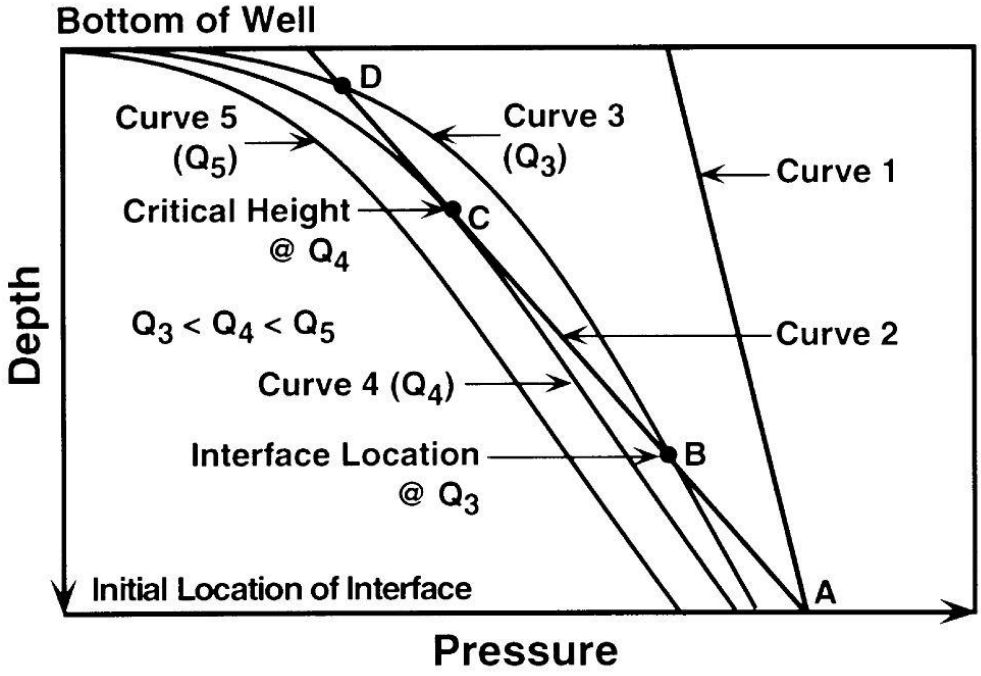

Figure 2.3. Freshwater and saline water pressure distributions under pumping conditions [19]

Although the Ghyben-Herzberg solution was a widely-applied method for approximating solutions for a sharp interface model, it needs to be adopted with careful evaluations because: (I) it neglects the non-uniformity of the aquifer, for example heterogeneity, (II) it neglects the movement of lower saline water, and (III) it neglects the thinning of freshwater zone due to the moving of interface. So many studies improved analytic solutions of SU by eliminating same of these assumptions. For example, Dagan and Zeitoun [25] considered the heterogeneity of an aquifer by analytically solving the interface flow in a stratified aquifer. Without the Dupuit assumption, Dagan and Bear [17] used the method of small perturbation to generate equations indicating evolution of the interface rise in two-dimensional and three-dimensional aquifers. Schmorak and Mercado [15] used the equation from Dagan and Bear [17] for upconing in a relatively thick aquifer for a field study of SU. The equation reads:

$$X(r,t) = \frac{Q}{2\pi\left(\frac{\Delta\rho}{\rho}\right)k_x d} \cdot \left[\frac{1}{(1+D^2)^{1/2}} - \frac{1}{[(1+T)^2+D^2]^{1/2}}\right], \tag{2.2}$$

where D and T are:

$$D = \frac{r}{d}\left(\frac{k_z}{k_x}\right)^{1/2}, \tag{2.3}$$

$$T = \frac{(\Delta\rho/\rho)k_z}{2nd}\mathrm{t}\,, \tag{2.4}$$

X is interface rise due to pumping, Q is pumping rate, $\Delta\rho$ is density difference between saline water and freshwater, ρ is density of freshwater, k_x and k_z are horizontal and vertical permeability respectively, d is distance from bottom of well to the initial interface, r is radial distance from the well, n is porosity, and t is time elapsed since start from pumping. In Equation. 2.2, the interface rise linearly increases with the discharge rate, consistent with steady-state upconing indicated before; however, if unsteady state occurred, when the interface rises abruptly, the linear

relationship no longer exists. So the applicability of the equation is limited under a threshold distance of interface rise, and through the experimental results in Dagan and Bear's research, the threshold value was found to be one third of the distance from initial interface to the sink. This was further validated in the field [15], numerical solutions [26] and physical experiments [27]. However, due to the method used, the equations were limited for the case that the deviations from an initially assumed steady interface should be small enough. Another example without Dupuit assumption is Nordbotten and Celia [28], who presented solutions for a sharp interface model with significant vertical flows considered, such as the region around the well. When considering both saline water and freshwater are moving, Bakker [29] provided an exact solution capable to generate the instantaneous flow fields in freshwater and saline water.

A sharp interface model was also solved using numerical computational methods, such as boundary element method, with full considerations of non-linearity of boundary conditions at the interface [e.g., 30, 31]. Reilly and Goodman [12] also included a sharp interface model implemented by numerical code SUTRA, for the primary purpose to compare the solutions of a sharp interface model and a variable-density flow model. The generally-used assumption that the sharp interface is a representative for the 50% isochor of a variable-density flow model was found only true for limited conditions, for example under a low pumping rate. Moreover, they obtained that even though the sharp interface was under steady-state, locating below the bottom of well, well salinity in a variable-density flow model was monitored. Such a phenomenon was due to hydrodynamic dispersion allowed in a density-dependent model, so that adopting a sharp interface model for SU predictions may lead to inaccuracy.

2.1.2 Variable-density flow model

Sharp interface models serve as an efficient way to estimate SU quickly. Variable-density flow models considering hydrodynamic dispersion are closer to practical situations. The hydrodynamic dispersion controls the physics of solute spreading. The governing equations for a variable-density flow system consists of (I) Darcy's law, (II) the equation of mass conservation, (III) the solute transport as a balance of advection, molecular diffusion and pore-scale dispersion, and (IV) the state equation. In a variable-density flow model, the SU is represented by a saline water plume. For example, Zhou et al. [8], who adopted a variable-density flow model for understanding detailed mechanism of upconing and decay processes, described the SU as two distinguishably separated regions: (I) the upconing region, where varied saline isochor obviously move upward to the well, and (II) the far away region, where varied saline isochor nearly stay horizontal. This is different from the upconing phenomena in a sharp interface model, as indicated in the Figure 2.4. Studies with a variable-density flow model are mainly focused on studying the mechanism of SU process.

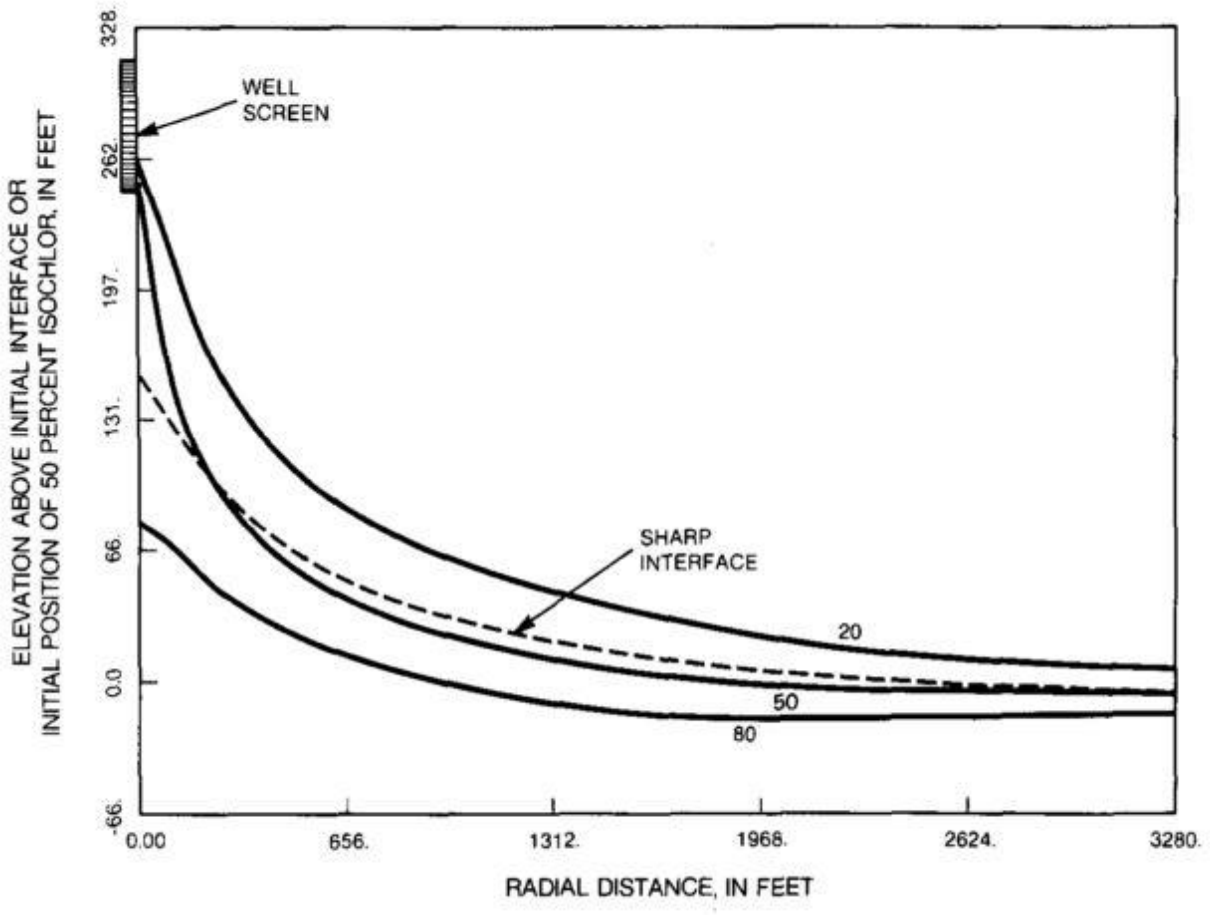

Figure 2.4. Interface rise due to pumping in a sharp interface model and a variable-density flow model [12]

Due to the recent fast improvement in computational power, many computer codes are available to solve a variable-density model of SU. These serve as important tools, as they are capable to mimic realistic hydrogeological conditions. Table 2.1 summarizes the major codes used in the literature, and their corresponding applications. SEAWAT now is the mainstream computer code. It is based on the finite-difference method and developed by USGS for simulating variable-density flow and solute transport in porous media [32]. It is developed by combining MODFLOW and MT3DMS into a single program that solves the coupled flow and solute transport equations

respectively. The governing equation of variable-density groundwater flow is expressed in terms of equivalent freshwater head, and the density is empirically linearized with the concentration in SEAWAT.

The highly coupled equations for a variable-density flow model are solved in these codes commonly by finite elements or finite differences. While these numerical methods work well for the flow equations, they can cause numerical dispersion for the solute transport, especially around the mixing region [6]. Shalabey et al. [33] used a varied form of method of characteristics (treating the precomputed volume of advective solute as a new source/sink to cause dispersion) for solving the solute transport numerically, which may require a longer run time. There is usually a compromise between the computational times and numerical accuracy. To consider that, a widely-used method is the adoption of a two-dimensional axisymmetric model, especially for SU in a local scale, which could be 1000 times faster than an equivalent 3D model [9]. A general 2D axisymmetric model conceptually representing SU is presented in Figure 2.5 [34]. The freshwater is in the upper region (blue color), while the lower part is occupied by saltwater (red color), and the interface (transition zone, green color) between them is initially horizontal. A level of discretization in an axisymmetric model is relatively simple, and a grid resolution analysis can be conducted by testing different levels of discretization. However, limitations also exist when adopting such a model. For example, an axisymmetric model cannot include the regional flow that may affect the extracted water salinity [34].

Table 2.1. Applied numerical codes in the literature and their well-known examples

SU Code	Applications
SUTRA	Voss and Kotch [35], Aliewi et al. [36], Reilly and Goodman [12]
FEAS	Zhou et al. [8]
SEAWAT	Marandi and Vallner [37], Cai et al. [38], De Louw et al. [39], Pauw et al. [26]
FEFLOW	Jakovovic et al. [34]

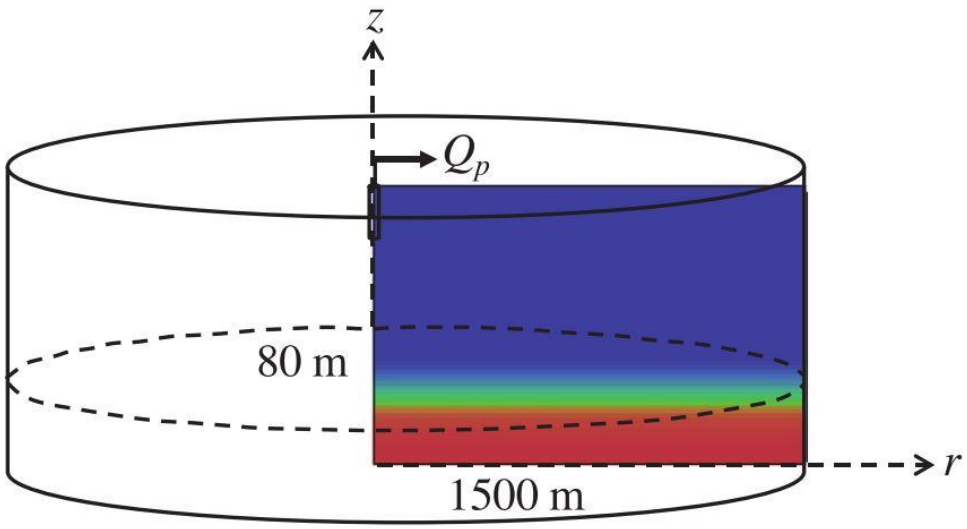

Figure 2.5. A typical axisymmetric model for numerical simulation of SU [34]

Numerical results usually require a benchmark process to verify its reliability. Three typical benchmark problems for the variable-density flow are the Henry problem [40], Elder problem [41] and Hydrocoin problem [42]. While they have been included in many numerical studies for problems including variable-density flows (for example, the Henry problem for SWI problem [e.g., 43, 44]), there are fewer studies using these benchmark problems under a specific SU scenario.

Oswald and Kinzelbach [45] proposed a physical benchmark to help to test the reliability of existing numerical codes (refer to Section 2.2). The experimental setting was similar to a local upconing process due to pumping. In their research, the code FEFLOW was tested, and it failed to predict the results when concentration gradients between freshwater and saline-water were high. One example of using these experimental data is the research by Johannsen et al. [46]. Using the program package d^3f, they successfully reproduced experimental results after some modifications of parameters (porosity, hydraulic conductivity and transversal dispersivity). Similarly, Jakovovic et al. [47] used the numerical code FEFLOW with a two-dimensional model to verify the experimental results from Werner et al. [27]. With minimum calibrations of parameters, FEFLOW reproduced the transient behavior of salt plumes from physical observations, even for the scenario with relatively high dispersive situation. So they concluded that the existing numerical code is able to model a density-dependent flow to a reasonable degree.

Applying numerical models based on realistic hydrogeological conditions to investigate SU is also a topic of interest, especially because field investigation of SU are still difficult to apply. Included in Reilly and Goodman [12], a numerical simulation of the salinity distribution under a pumping well at Truro, Massachusetts (Test Site No. 4) was performed, and the variation of on-site and simulated Chloride concentrations suggested that the local aquifer should have a very small transverse dispersivity. Ma et al. [48] developed a 3D numerical model for an unconfined aquifer based on the site condition in Siefkes, USA to test the impact of uncertainties of hydrogeological parameters on SU, and they concluded that key parameters affecting SU were existence of clay layer, depth of well screen, hydraulic conductivities of the aquifer, and pumping rate. Voss and Koch [35] studied SU occurring in the shallow lowlands of the state of Brandenburg, Germany, where the surface river induced the natural SU in that shallow aquifer.

They tested the significance of the density-dependent model for such a process, and concluded that a passive transport with less computational effort was sufficient for the prediction. Aliewi et al. [36] used the numerical code RASIM [49], and SUTRA for operations of controlling wells (skimming well and scavenger well) on SU in Jerico area and Gaza area of Palestine respectively. They concluded that scavenger wells operated more effectively in terms of preventing discharge of saline-water. Marandi and Vallner [37] developed a 3D numerical model for the upconing behavior of Cambrian-Vendian aquifer system in Estonia. The model was calibrated by the historical measurements in terms of water head and TDS concentration, and they concluded the significance of depths of well screens to control salinity level of pumped water. De Louw et al. [39] used numerical models for the natural upconing process occurring in Dutch deep folders (refer to Section 2.3). The numerical models simplified the hydrogeological conditions of the site, with the purpose to examine whether a simplified numerical model was sufficient for representing a real upconing process, and sensitivity analysis was applied to find out the dominant parameters and mechanisms. It was found that the error between the simulation results and field measurements was at a small scale, and the boil discharge, horizontal hydraulic conductivity of the aquifer, depth of mixing zone and salinity contrast between fluids served as the sensitive parameters for SU. The regional flow, barely included in previous studies, was found possible to impact the boil salinity, depending on the relative location of mixing zone to the regional flow. Cai et al. [38] developed a 2D numerical model to evaluate the pathways for upconing of deep saline groundwater occurring in southwestern Berlin, Germany, and the windows existing in Oligocene clay due to glacial erosion was found to be the reason.

There are few studies available to include the mixing behavior analytically. This research topic is not without significance when many numerical codes are available. This is because the

Peclet number (P_e) as the primary parameter describing the SU is found to be large (P_e = O (10^3 – 10^4) under some conditions [e.g., 12, 50]; this means a thin mixing zone may exist between fluids. This kind of problem is difficult to be achieved in numerical codes, because a very high level of discretization near the interface is necessary. Given that, analytically solving the density dependent problem is of interest; however, this does not mean to simultaneously solve the above coupled equations, but it was achieved either empirically or still with some assumptions. Bear and Todd [51] proposed a method to analytically superimposed the hydrodynamic dispersion if the upconing process was assumed one-dimension upward movement, and the abrupt interface represents the center of the transition zone (c = 50%). The solution can be expressed as

$$c = \frac{1}{2} erfc\left(\frac{Z - Z_{rise}}{\sqrt{2}\sigma}\right), \tag{2.5}$$

where c is the normalized concentration, defined as $(C - C_f)/(C_s - C_f)$, Z is the initial interface, Z_{rise} is the interface travelled distance, and σ is half of the transition zone and defined as $1/2[Z_{c=0.159} - Z_{c=0.841}]$. This method of superimposing the dispersion was used in the research by Schmorak and Mercado [15], Wirojanagud and Charbeneau [16] ,and Pauw et al. [26] incorporated with a sharp interface solution. Through comparison with numerical results, Pauw et al. suggested that this method was not appropriate for prediction of well salinity.

Paster and Dagan [52] suggested the boundary layer approximations for the aquifer with large P_e. The boundary layer equations were generated for a homogeneous isotropic axisymmetric flow problem [52] and a 3D regional flow problem in a confined coastal aquifer [53], and they were used for pumping under a local and regional scale respectively. The salinity of pumped water could be generated. However, these boundary layer approximations was not validated by other methods, so that to what extent it is correct needs future investigation.

More recently, Pool and Carrera [54] introduced an empirically correction factor in terms of transverse dispersivity and aquifer thickness to the original Strack's equation to account for the mixing between seawater and freshwater. This was achieved by comparing the results of Strack's equation [21] with numerical results from SUTRA through an optimal regression model. They also concluded that the sharp interface model could underestimate the critical pumping rate for a fully penetrating well in coastal aquifer. The modified Strack's equation could obtain consistent results to a variable-density flow model in numerical solutions, in terms of the critical pumping rate.

2.2 Laboratory scale physical models

Physical models in laboratory settings can provide reliable data for understanding the mechanisms of SU, and benchmark existing mathematical solutions, while field investigations still hold operational difficulties. Generally, two types of experimental settings are examined: a local upconing setting (initially horizontal interface between two fluids), and a regional setting with SWI (initially inclined interface between fluids).

Dagan and Bear [17] seem to be the first to perform a laboratory experiment of SU. The main purpose of their experiments was to validate the theoretical expression they developed. Therefore, the variable of interest is the critical interface, and thus they just summarized the rise of average interfaces as their experimental results. Werner et al. [27] extended these experiments by conducting a series of lab experiments to provide transient physical observations of a dense saline plume due to local pumping. Figure 2.6 presents one of their experimental results (experiment 1 with high pumping rate and low density difference). It shows that, generally, the experimental behavior of saline plume is a 'dispersive to nondispersive' process (especially from

Figure 2.6(c) to Figure 2.6(f)). This could be because the longitudinal dispersion dominates the early stage of solute transport, and the smaller transversal dispersion controls the transport when the lower isochor intercepts the well. These experimental results were also compared with the theoretical solution of Dagan and Bear [17], and were validated numerically by Jakovovic et al. [47]. Adopting the analytic solution showed that, in general, for the scenario with high pumping rate where the dispersive process was less dominant, the analytic solution can well approximate the rise of saline plume during its early stage. In the study by Jakovovic et al. [47], most of the experimental results were reproduced, except for their experiment 4 with an unexpected double peak of saline plume. This was explained as the impact of adsorptive feature of the Rhodamine WT tracer used in experiments [55]. The low pumping rate led to significant spatial variations of velocities in the saltwater plume, increasing from the plume center to its edge, so that the tracer moved with a faster flow along the edge of plume, leading to the observed double-peaks. Based on the setting of the typical Hydrocoin problem [42], Oswald and Kinzelbach [45] conducted a series of laboratory experiments in three-dimensions. Their study's aim was to collect reliable and sufficient data of salt-mass distributions for varied spaces and time-scales under a controlled laboratory settings, for the ultimate purpose to propose a benchmark problem for exiting numerical codes. It was suggested that numerical results can be verified against the experimental data in terms of two characteristic diagrams: concentration distributions in the diagonal cross-section and breakthrough curves for water discharged.

More recently, Mehdizadeh et al. [56] conducted a sand-tank experiments of upconing below a partially penetrating well in a regional setting with SWI to examine the accuracy to assume the immiscibility between two fluids. They compared the results regarding the saltwater wedge shape and well salinity from the lab experiments and the sharp interface solution, and they

concluded that the sharp interface approach overestimated the toe position (compared with the 50% isochor), but underestimated well salinity.

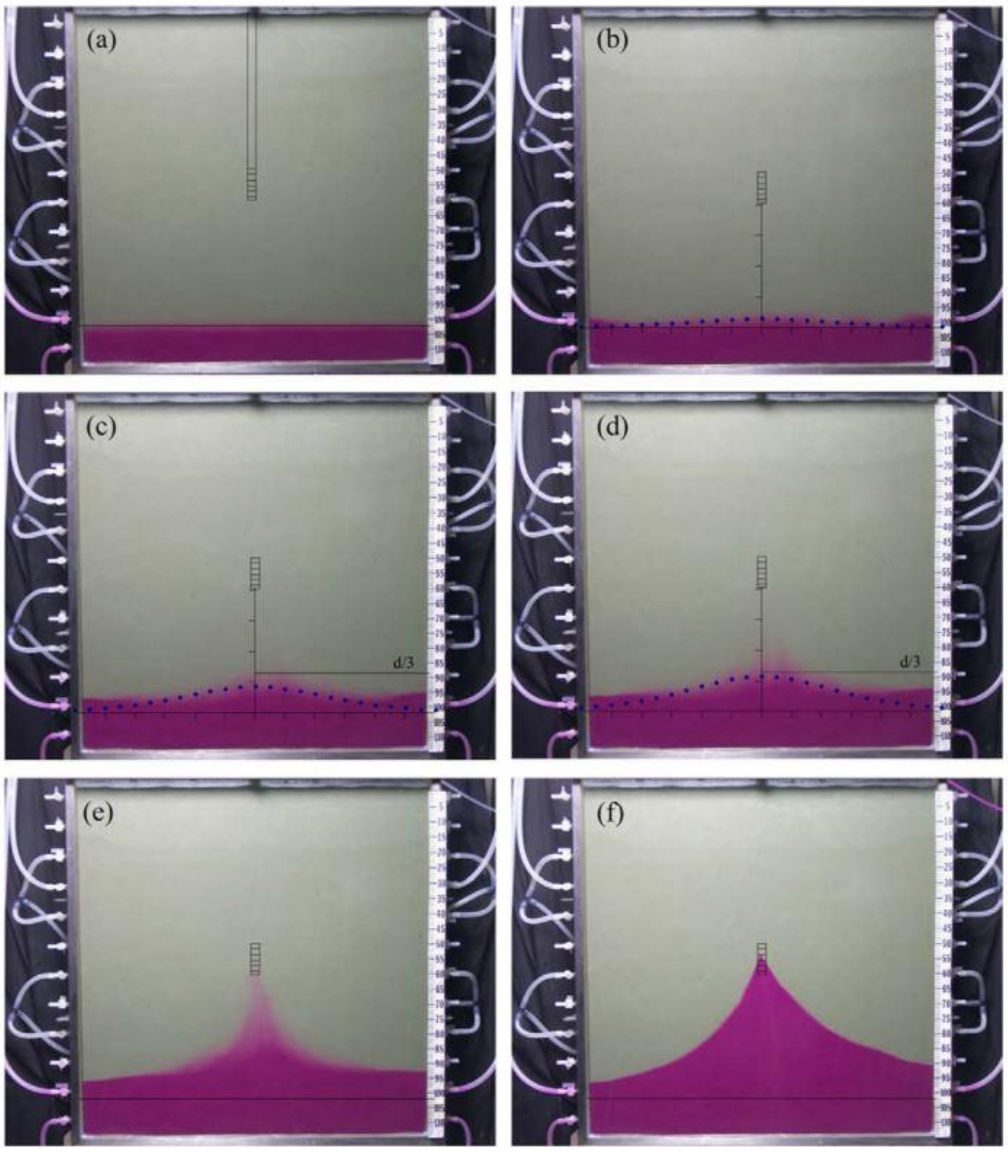

Figure 2.6. An experimental result for SU under high pumping rate and low density difference [27]

2.3 Field investigation

The major difficulty of field investigation of SU is the evaluation of solute transport processes at field scale. Currently, this is mostly achieved by recording the value of Electrical Resistivity (ER) or its reciprocal value Electrical Conductivity (EC) in localized monitoring wells. For example, Schmorak and Mercado [15] seem to be the first ones to have measured the SU in the field. They studied the site with upconing in the Ashqelon area of Israel, and recorded ER values in 4 monitoring wells for the salinity profiles corresponding to different discharge rates and durations. Their primary aim for field investigation was to evaluate the existing analytic solutions for SU (refer to Section 2.1.1). De Louw et al. [39] used a similar method for the natural upconing process occurring in Dutch deep folders. That study site was found with varied salinities, and in their previous work [57], they concluded that the dominant mechanism was the preferential groundwater discharge through boils. Boils were developed at site due to the conduits formed between surface water and groundwater, when the water pressure in the underlying aquifer is larger than the pressure induced by the weight of the overlying stratum. They adopted a linear relation between CL concentrations and EC (i.e. CL = 0.36EC – 0.45 [58]). The resultant CL concentrations showed an obvious saline upconing towards the boil. Similarly, a regional upconing profile for a site in the Spanish Mediterranean coast was generated through recording EC values among 34 irrigation wells [59]. The study area has experienced a heavy loading of pumping for agricultural usage in the mid-1990s. Numerous wells were constructed during that time, but the intrusion of salt wedge had caused most of them to be abandoned. The recorded EC values showed good correlation to the recorded CL concentrations. So it could be concluded that using the EC value can well predict geometry of SU at field scale. The widely used technology Electrical resistivity tomography (ERT) was used by Kura et al. [60] for the response of salinity distribution

to pumping in Kapas Island, Malaysia. The imaginary salinity distributions they obtained showed obvious upconed saline-water after pumping. They also noticed that intensively dilution of saltwater with freshwater occurred when recovery process began, causing a larger area of groundwater with low-salinities. They validated their results by comparing the resistivity values from field monitoring with the values from soil matrix samples in the laboratory experiment.

2.4 Research gap

SU has been investigated for over nearly 60 yrs. Its study started during the early stages with sharp-interface approximations to focus on its critical conditions. Later, numerical solutions considering the density effects were increasingly studied, and with the advancement of computational power, numerical codes were developed and made available for variable density flow problems. This development boosted studies focusing on mechanisms controlling SU. Meantime, laboratory scale physical experiments for SU became available. All these studies revealed that rate and extent of SU rely on many factors, such as hydraulic properties of the aquifer, pumping rate and duration, initial interface position, density contrast between freshwater and saltwater, and regional flow. Additional factors are dispersion and sorption effects, groundwater recharge, and the well and aquifer geometries. Field studies of SU were limited to physically confirm the phenomenon of SU at a site due to the difficulties to monitor the transport of solutes at field scales.

While the impacts of many parameters have been tested, there is very limited research investigating the impact of aquifer heterogeneity on the SU processes neither adopting numerical models nor physical models. To my knowledge, the only study of SU in heterogeneous aquifers is

the analytic research by Dagan and Zeitoun [25]. However, the importance of inherent aquifer heterogeneity on variable-density flow has been highlighted by a number of studies [e.g., 6, 7]. Therefore, this study is motivated to numerically investigate the impact of aquifer heterogeneity on the SU process.

Chapter 3

IMPACT OF A LOW-PERMEABILITY LAYER ON THE PUMPING EFFICIENCY UNDER THREATS OF SALTWATER UPCONING

A multilayered aquifer is a typical geological formation in a real situation. The lateral intrusion of saline water (i.e. SWI) in such a formation was studied in the literature, which was mainly achieved by adopting numerical or physical models with a single or several horizontal layers showing distinguished permeability [e.g., 61, 62, 63]. Taking a recent research by Lu et al. [61] as an example, they investigated the steady-state mixing zone development due to SWI in stratified coastal aquifers, which were achieved by dividing the whole model domain into three horizontal layers. They assigned a range of values of hydraulic conductivities to these layers, and both numerical modelling and laboratory experiments were included. They observed that a low-hydraulic conductivity (*K*) layer exerts a high impact on the mixing zone developments. Accordingly, we hypothesize that the presence of a low-*K* layer would highly affect SU dynamics.

Therefore the main aim of this chapter is to investigate the impact of a low-*K* layer on SU processes using a variable-density flow and solute transport numerical model, as a first step to analyze the effects of aquifer heterogeneity on the generation and dynamics of SU. The pumping duration, the same definition as in Zhou et al [8], will serve as the main indicator for assessing the impact of the low-*K* layer on the pumping efficiency. The results of layered aquifers and corresponding homogeneous aquifers will be compared to reveal the importance of the low-*K* layer on controlling groundwater flow and salt transport. More importantly, quantitative relationships between the pumping duration and the *K* magnitude of the low-*K* layer are obtained; these provide

a simple tool for developing natural and artificial barriers to prevent saltwater up-coning and enhance the pumping efficiency.

3.1 Method

3.1.1 Conceptual model and parameter values

The conceptual model in Zhou et al.[8], modified from the saltwater up-coning problem presented by Reilly and Goodman [12] and Voss and Souza [64], is further modified in this study and is used as a reference case, since the aquifer is heterogeneous (Figure 3.1). An axisymmetric, anisotropic, and confined aquifer is considered; the domain with a radius of 3000 m and 150 m thickness, initially consists of three zones identified by different concentrations. The upper zone is the freshwater zone (C_f = 0 kg m^{-3}) and 98 m thick, while a 50 m thick saltwater zone is located at the bottom of the aquifer with the concentration C_s = 35 kg m^{-3}. A 2-m thick mixing zone separates these two zones with a concentration equal to C_s/2. The origin of the coordinate system is located at the bottom left of the model domain. In comparison with the conceptual model used in Zhou et al. [8], the thickness of the saltwater zone is increased from 20 to 50 m, and the radius of the model is increased from 2000 to 3000 m. These modifications were necessary to assure that the saltwater zone was deep enough to be able to supply water for length of all simulations. A smaller domain would have caused the concentrations of the water near the bottom boundary to become lower than C_s, this affecting the pumping times, which was observed in simulations in this project when adopting the exact domain size from Zhou et al.

An extraction well was located at the center of the axisymmetric domain at the top of the freshwater zone with a constant pumping rate Q_u= 2,400 m^3 d^{-1} and a well screen length d_f = 20 m. The initial hydraulic head is set as 10 m above the aquifer top. Recharge of freshwater and

saltwater occurred along the external radial boundary with fixed-head (also 10 m above the aquifer top) and fixed concentration boundary conditions. Note that the fixed concentration is used in solute boundary condition, while in Zhou et al., a concentration gradient of zero is prescribed normal to the boundary, and therefore salt can enter from this boundary only through advection. After pumping, saline water beneath the well is gradually drawn upward and the concentration of the extracted water gradually increases. Like in Zhou et al., it is assumed that, once the concentration of the extracted water reaches 2% of the saltwater concentration (i.e., C_s), the well is shut off.

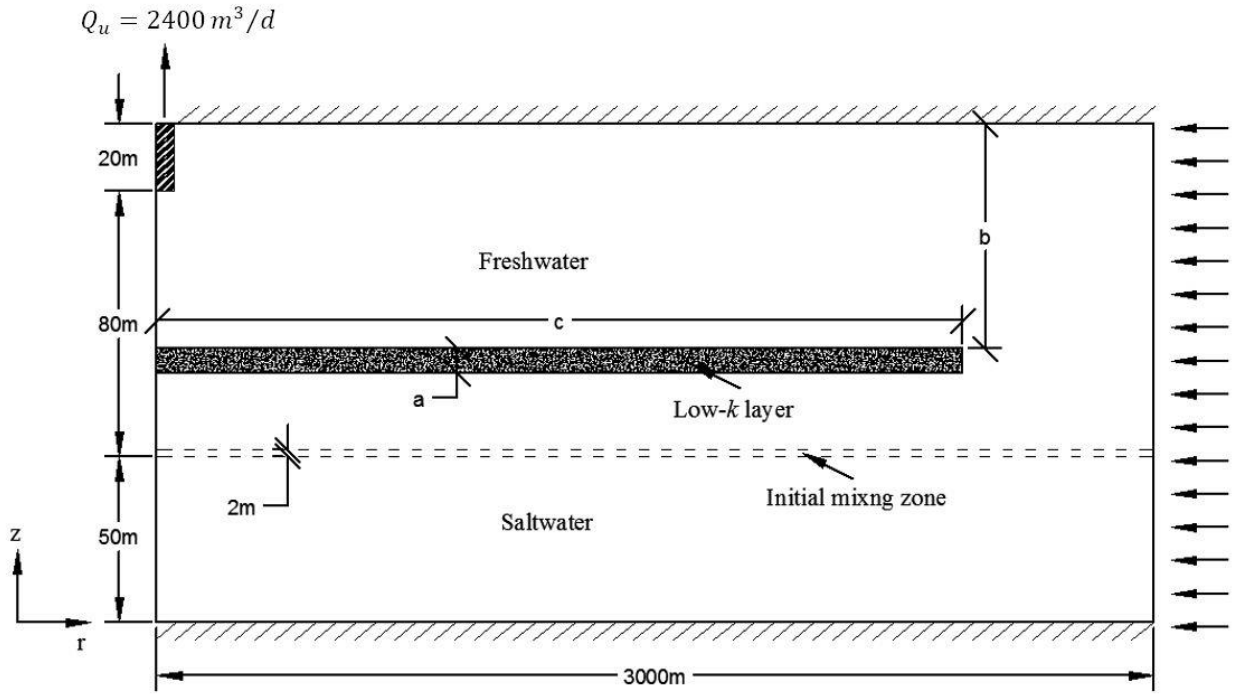

Figure 3.1. Conceptual model of a saltwater upconing problem (modified from Figure 1 in Zhou et al. [8])

For the base homogenous case, permeability in the horizontal and vertical directions (k_x and k_z) are 2.56×10^{-11} and 1.0×10^{-11} m^2, respectively. A constant value of 1×10^{-3} kg m^{-1} s^{-1} is

used for dynamic viscosity (μ). The porosity (θ) of the aquifer is 0.2. The densities of the freshwater (ρ_w) and saltwater (ρ_s) are 1000 and 1025 kg m^{-3}, the latter approximately equaling to a common density of seawater. The longitudinal and transversal dispersivity (α_L and α_T) are 1 and 0.5 m, respectively. Molecular diffusion is neglected. The values of the parameters in the homogeneous case, listed in Table 3.1, are as those assumed for Case A in Zhou et al.

To study the effect of layered aquifer heterogeneity on SU, a horizontal low-*k* layer is considered with a thickness of *a*, distance between the top of the low-*k* layer and the top of aquifer of *b*, and extent from the well *c*. By varying the values of *a*, *b*, and *c*, more scenarios are designed to test their sensitivity. Three different values of *a* (2, 4, and 8 m) are selected. For *b*, five values (6, 20, 32, 46, and 50 m) are chosen; when *b* = 20 m, the low-k layer locates exactly below the bottom of extraction well. Six values of *c* (100, 500, 1000, 1500, 2000, and 3000 m) are assumed, where *c* = 3000 m means that the low-*k* layer extended to the entire length of the domain. Moreover, to examine the sensitivity of the *k* magnitude of the low-*k* layer, values ranging from one to three orders of magnitude lower than the value in the homogeneous case are adopted. The highest values of *k* correspond to sands and the lowest values silts [65]. When varying the value of *k*, the anisotropic ratio is fixed.

Table 3.1. Values of parameters in the homogeneous case

Parameter	Symbol	Value	Unit
Porosity	θ	0.2	-
Permeability in the horizontal direction	k_x	2.56×10^{-11}	m^2
Permeability in the vertical direction	k_z	1.0×10^{-11}	m^2
Dynamic viscosity	μ	1.0×10^{-3}	kg m^{-1} s^{-1}
Pumping rate	Q_u	2400	m^3 d^{-1}
Freshwater density	ρ_f	1000	kg m^{-3}
Saltwater density	ρ_s	1025	kg m^{-3}
Longitudinal dispersivity	α_L	1	m
Transverse dispersivity	α_T	0.5	m
Molecular diffusion coefficient	D_m	0	m^2 s^{-1}

3.1.2 Numerical implementation

Numerical simulations are implemented by SEAWAT-2000 [66]. Computer programs included in SEAWAT (i.e. MODFLOW and MT3DMS) are originally based on the Cartesian coordinate system. Langevin [9] showed that axisymmetric flow and transport can be simulated by these programs by adjusting several input parameters to account for the increase in flow areas with radial distance from the well, as simply expressed in Equation 3.1. In addition, the logarithmic weighting of inter-block transmissivity that is a standard option in MODFLOW can be used for axisymmetric models to represent the linear change in hydraulic conductance within a single finite-difference cell.

$$X_j^* = X_j \theta r_j, \tag{3.1}$$

where X_j is an aquifer property or transport parameter required adjustments since it is associated with flow area (e.g., hydraulic conductivities, specific storage and porosity), θ is the angle, set to 2π, r_j is the radial distance from the well, X_j* is the correspondingly adjusted parameters to X_j.

For the reference case, the entire domain is discretized into 75 layers and 307 columns, resulting in 23025 cells in total. Each layer is 2-m thick, while the columns are variably spaced with 0.25-m horizontal resolution near the well expanding to 25-m horizontal resolution at the radial boundary. This discretization scheme is similar to that used in Langevin.

3.1.3 Quantitative indicators

As mentioned above, the salt concentration distribution (C) and the pumping duration (T) before the salinity of pumped water reaches a specified value (2% in the current study) are taken as quantitative indicators. Here, we define two dimensionless variables based on these two indicators:

$$w = \frac{C}{C_s}, \tag{3.2}$$

and

$$E = \frac{\left(T_L - T_H\right)}{T_H}, \tag{3.3}$$

where T_L and T_H are the pumping durations when the salinity of pumped water reaches 2% in layered and homogeneous cases, respectively. E quantifies the efficiency of well pumping under the threats of saltwater up-coning. In addition, a dimensionless parameter β is defined to reflect the relative magnitude of k of the low-k layer to that in the homogenous case:

$$\beta = \frac{k_H}{k_L}, \tag{3.4}$$

where k_H and k_L are permeability of the homogenous case and the low-k layer in the horizontal direction, respectively. Since the anisotropy ratio of the aquifer is maintained the same for all

cases, the value of β is constant for a given low-k layer regardless of the direction of permeability.

3.2 Result and discussion

3.2.1 Impact on the flow field

Figure 3.2 shows the streamlines developed in the homogeneous aquifer case and layered aquifer case after 1, 2, 5, and 20 yrs., in which the layered aquifer has the parameters a = 2 m, b= 50 m, c = 3000 m, and β = 1000. The streamlines start from the external boundary with the vertical coordinates between 20 and 70 m. The streamlines in both cases change with the time, and the presence of the low-k layer alters significantly their direction. Initially, the streamlines near the external boundary in the homogeneous case are higher than in the layered case (see Figure 3.2a). With time the relative locations of the streamlines near the external boundary in the two cases are gradually altered (see Figures 3.2b-3.2d). On the other hand, the presence of the low-k layer cause the streamlines to go up earlier than the counterparts in the homogeneous case. It is interesting that at larger pumping times, the lower streamlines in both cases tend to arrive at the vertical axis with z = 95 m, though this occurs in the homogeneous case earlier.

Figure 3.3 shows the development of the flow regime in the homogeneous aquifer case and layered aquifer case (the same case as in Figure 3.2). Similar to the findings in Zhou et al. [8], who used a smaller domain, flow recirculation regimes are developed in both cases at the bottom-left saltwater zone during pumping though they occur at different times. Comparison with additional simulation results (not shown here) shows that the enlarged model domain used here results in the later occurrence of flow recirculation. The flow recirculation beneath the pumping well prevents

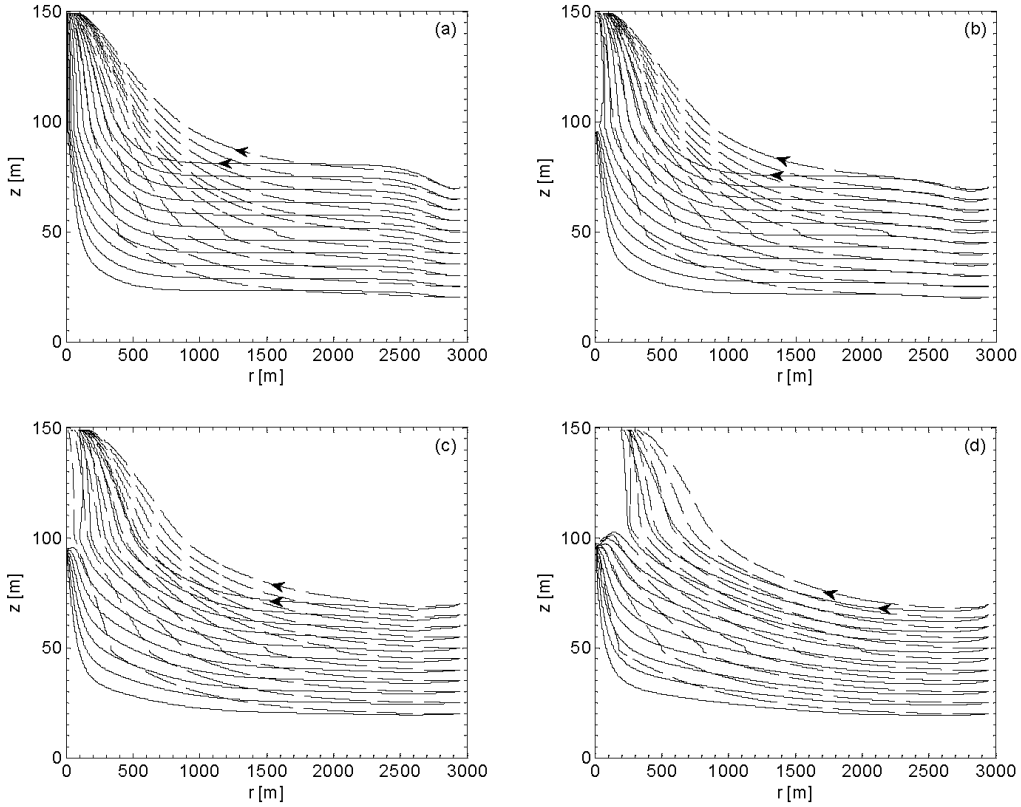

Figure 3.2. Streamlines developed in the homogeneous case (solid lines) and the layered case (dashed lines) after (a) 1 yr., (b) 2 yrs., (c) 5 yrs., and (d) 20 yrs.

the high concentration of saltwater in the mixing zone from migrating upward to the well (i.e., up-coning). It is shown that the flow recirculation regime in the homogeneous aquifer case is developed earlier than in the layered-aquifer case. On the other hand, the area of the flow recirculation regime in both cases grows with the time.

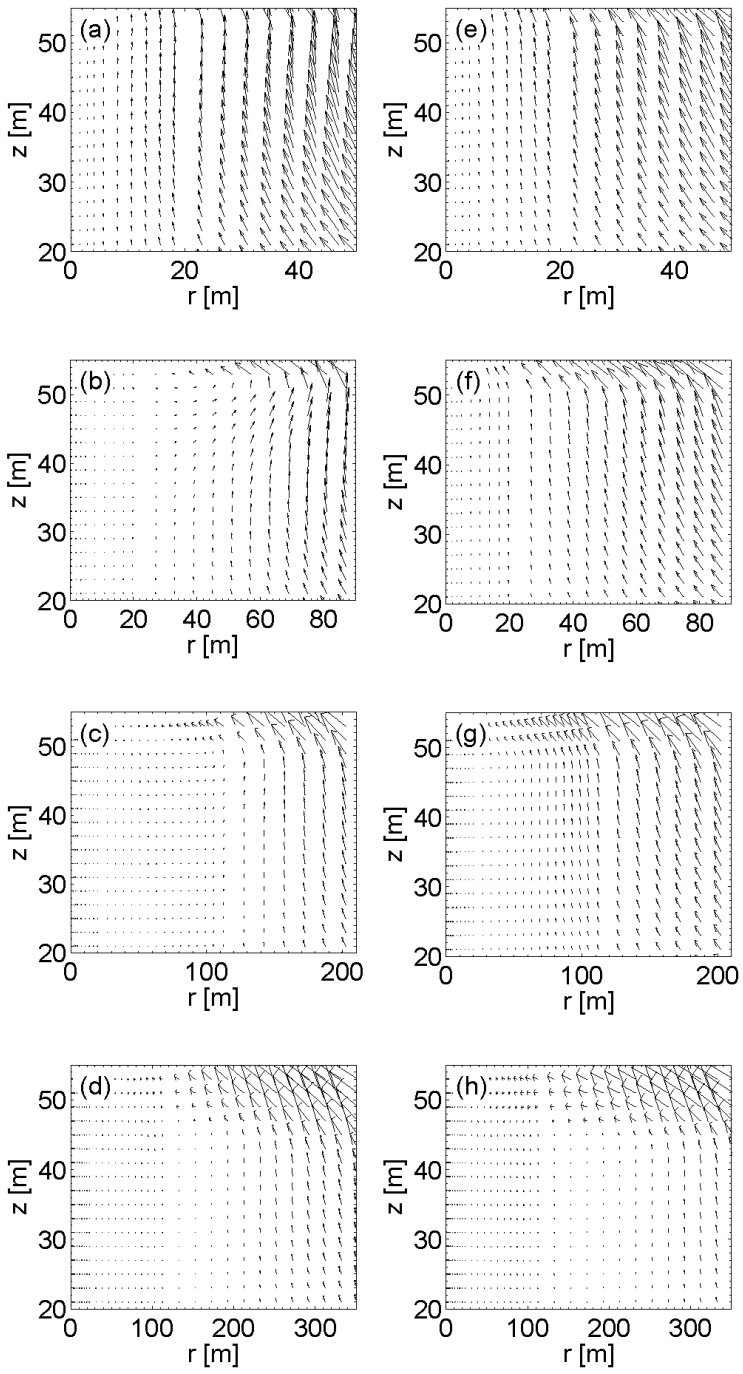

Figure 3.3. The development of the flow regime after 1, 2, 5, and 20 yrs. in the bottom-left saltwater zone in the homogeneous aquifer case (a-d) and layered aquifer case (e-h)

3.2.2 Impact on breakthrough curves of pumped water

Figure 3.4 shows the breakthrough curves of pumped water for the homogeneous case and layered aquifer case (the same case as in Figure 3.2). As shown, the rate of saltwater up-coning in the homogenous case is significantly faster than that in the layered case. For the layered aquifer case, during about the first 10 yrs., there is no obvious response of the concentration of pumped water to well pumping, while only about 300 days are found for this phase in the homogeneous aquifer case. The values of T_H = 5.2 yrs. and T_L = 46.7 yrs. result in a value of E = 8.0 (Equation 3.3). The value of T_H in the current study is smaller than 5.6 yrs. in Langevin [9]. With the larger model, saltwater is supplied by the aquifer near the well leading to lower pumping times. With the size of the domain used by Zhou et al. [8] and Langevin, the saltwater layer at the bottom of the aquifer is not deep enough and salty water is thus replenished from the external lateral boundary on the right leading to longer pumping times.

3.2.3 Impact on the increment of the total salt mass

Figure 3.5 shows the transient increment of the total salt mass within the model domain for the homogeneous case and layered aquifer case (the same case as in Figure 3.2). During approximately the initial 6 yrs., the two curves in the figure are almost overlapping, indicating that the increment of the total salt mass for the two cases are very close, despite of the significant difference of the average salt concentration of pumping water in the two cases (see Figure 3.4). In other words, the impact of the low-*k* layer on the increment of the total mass within the model domain during this initial stage is not significant. After that, the curve of the homogeneous aquifer case deviates from that of the layered aquifer case, representing that the increment of the total salt mass in the former case is obviously larger than that in the latter case.

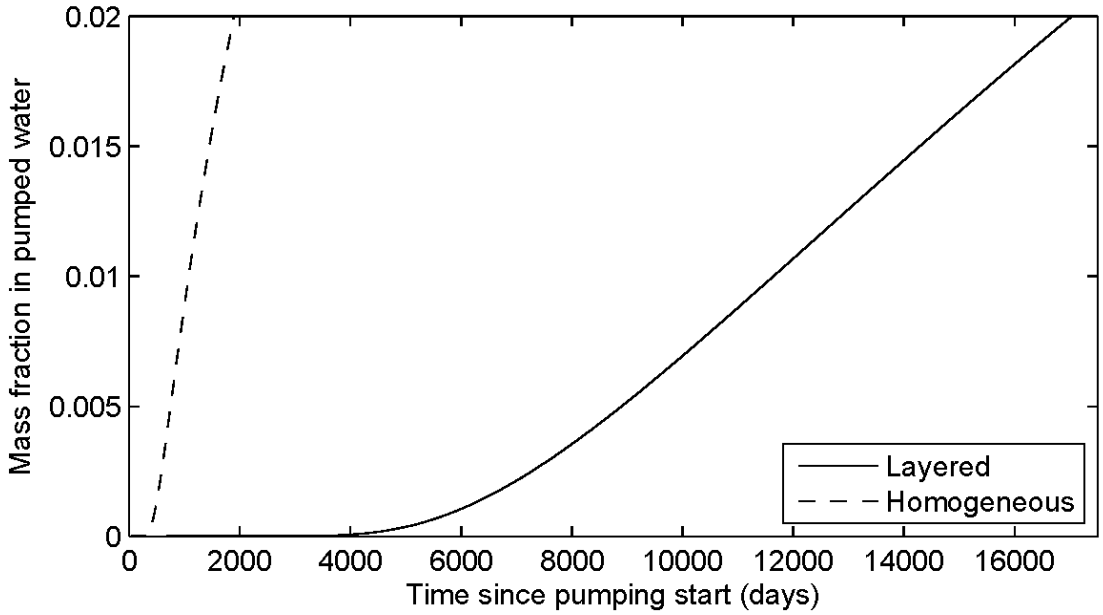

Figure 3.4. The breakthrough curves of pumped water in terms of average pumping water salinity for homogeneous (dashed line) and layered (solid line) cases.

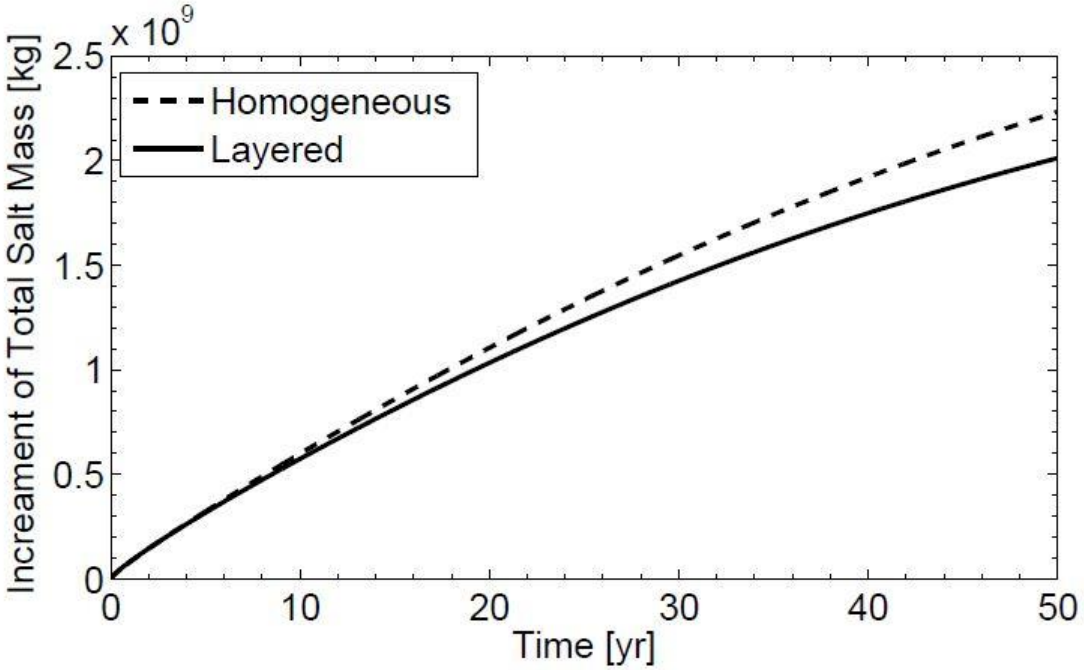

Figure 3.5. The breakthrough curves of increment of total salt mass within the domain for homogeneous and layered cases.

3.2.4 Impact on the salt concentration distribution

Figure 3.6 shows transient salt concentration distributions after 1, 3, 5.2, and 46.7 yrs. of pumping in the homogeneous case and layered aquifer case (the same case as in Figure 3.2). The salt concentration distributions are characterized by five contour lines of the normalized mass fraction (w = 0.02, 0.2, 0.5, 0.8, and 0.98). One can find from these figures that the concentration contour line w = 0.98 is very close to the concentration contour line w = 0.8 and only slightly lower than its initial position even at large pumping times; this indicates that the thickness of the saltwater layer adopted is sufficient to replenish the up-coned saltwater. This would not occur with the domain used in Zhou et al. [8] and Langevin [9] (not shown here).

After 1 yrs. of pumping, the salt concentration distribution below the pumping well in the homogeneous case is visibly affected, while negligible effects on the layered aquifer case are found; this shows that the low-k layer exerts a significant impact on preventing saltwater up-coning (Figures 3.6a and 3.6e), as expected. When the well has pumped for 3 yrs., the mixing zone (defined as the zone between the concentration contour lines of w = 0.02 and 0.98) in the homogeneous case is widened significantly and the concentration contour line of w = 0.02 enters the well (Figure 3.6b). However, the average concentration of pumped water has not reached the criterion of well shut-off. At the same moment, by contrast, the mixing zone is slightly widened and the salt concentration distribution starts to ascend in the layered aquifer case (Figure 3.6f).

When the well has pumped for about 5.2 yrs., in the homogeneous case, the mixing-zone thickness is remained similar and the four concentration contour lines of w = 0.02, 0.5, 0.8, and 0.98 are at similar locations, in comparison to those developed after 3 yrs. of pumping (Figure 3.6c). However, the concentration contour line of w = 0.2 has been elevated significantly, causing the average concentration of pumped water to reach the well shut-off criterion (i.e., T_H = 5.2 yrs.).

At this time, in the layered aquifer case five concentration contour lines are still below the low-*k* layer, although the thickness of the mixing zone is increased noticeably (Figure 3.6g). This indicates that the presence of the low-k layer slows dramatically the saltwater up-coning rate, and results in a longer allowable pumping time. The concentration of pumped water in the layered aquifer case reaches the well shut-off criterion when the well has pumped for about T_L = 46.7 yrs (Figure 3.6h). If the well shut-off criterion does not apply to the homogeneous aquifer case, the up-coning of saltwater is extensive and the aquifer is highly contaminated by saltwater (Figure 3.6d). Interestingly, at large pumping times, the highest concentration contour lines (i.e., w = 0.98) could be below the initial condition in both cases, further widening the mixing zone.

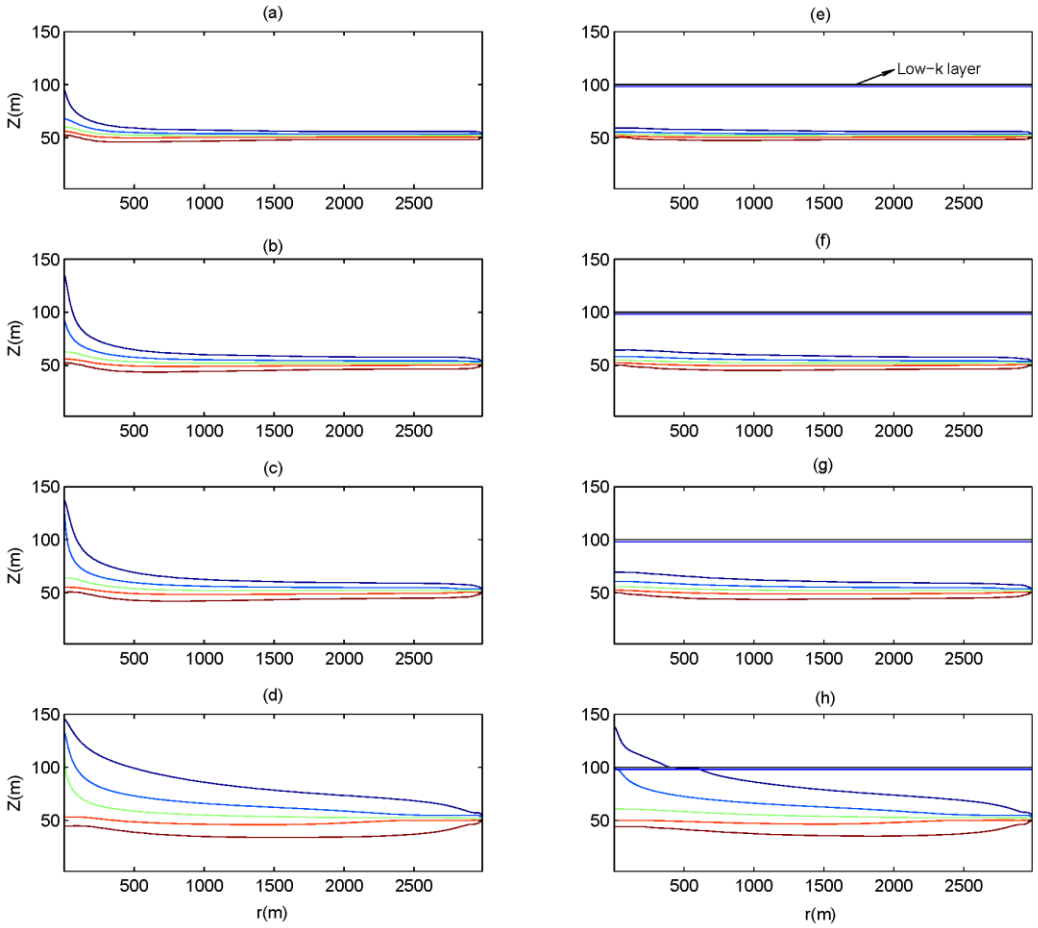

Figure 3.6. Transient salt concentrations after 1, 3, 5.2, and 46.7 yrs. of pumping in the homogeneous aquifer case (a-d) and layered case (e-h). For each salt distribution profile, from the top to the bottom are: 0.02, 0.2, 0.5, 0.8 and 0.98 isochor.

3.3 Sensitivity analysis

3.3.1 Sensitivity to *a* and *β*

Figure 3.7 shows that the sensitivity of E to β for a = 2, 4, and 8 m, with b = 50 m and c = 3000 m. Sound linear relationships are found for different values of a, with R^2 all equal to or larger than 0.988. A larger thickness of the low-k layer results in a higher value of E, as expected. In other words, a thicker low-k layer would facilitate preventing saltwater up-coning and increasing the pumping efficiency (i.e., E). When the low-k layer is 8 m thick and its permeability is three orders of magnitude less than that of the homogeneous aquifer, the allowable pumping duration is about 22 times higher than that of the homogeneous aquifer case (i.e., E = 22).

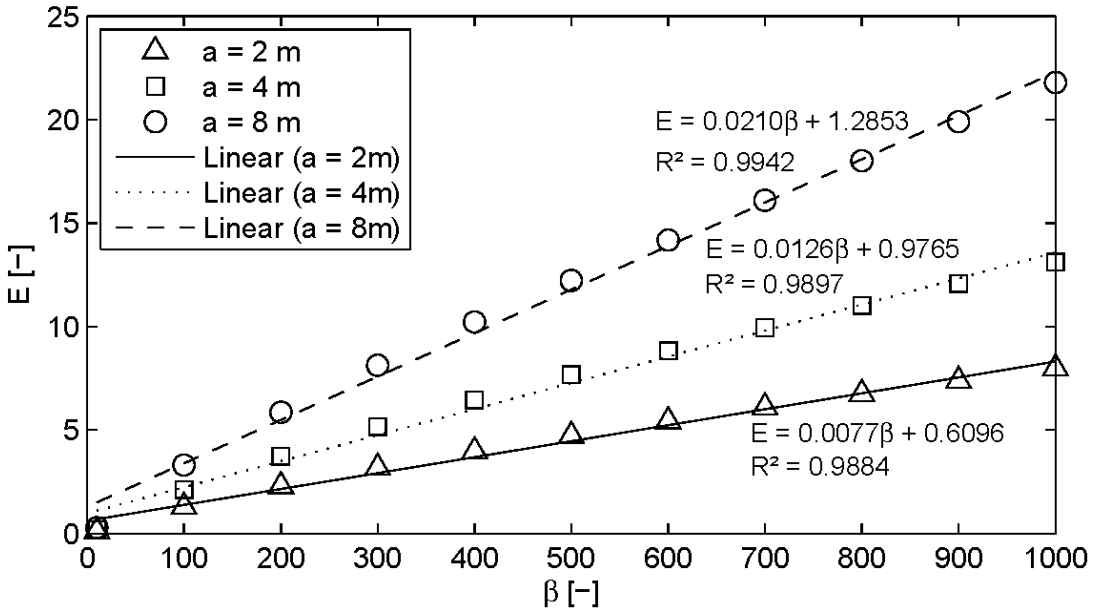

Figure 3.7. Sensitivity of E for a = 2, 4, and 8 m, with b = 50 m and c = 3000m.

3.3.2 Sensitivity to *b* and *β*

Figure 3.8 shows the sensitivity of *E* to *β* for *b* = 6, 20, and 50 m, and the sensitivity of *E* to *b* when *β* = 10, 100, 500, and 1000, in which *a* = 2 m and *c* = 3000 m. Good linear relationships are constructed between *E* and *β* for three different values of *b* (Figure 3.8a). It is clearly shown that *E* is not a monotonic function of *b* and the largest *E* occurs when the low-*k* layer is below and near the bottom of the well. By contrast, when the well penetrates the low-*k* layer, *E* decreases significantly with decreasing *b*. On the other hand, when *b*>30 m, *E* decreases gradually with increasing *b*.

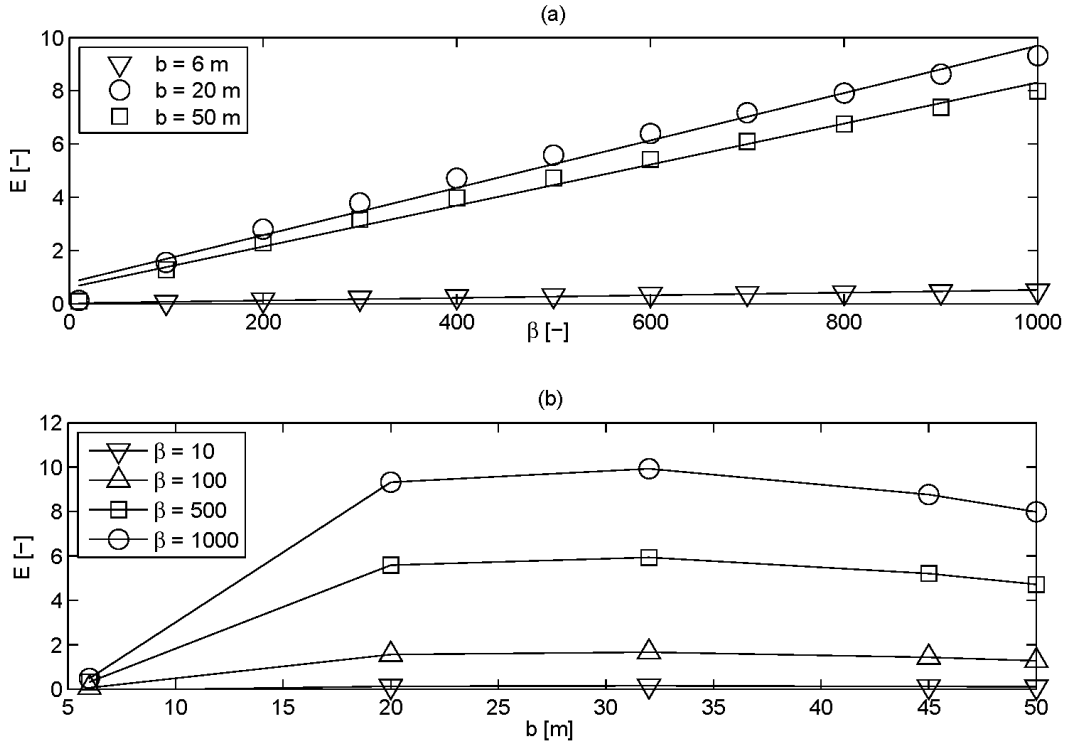

Figure 3.8. (a) Sensitivity of *E* to *β* for *b* = 6, 20, and 50 m, and (b) sensitivity of *E* to *b* for *β* = 10, 100, 500, and 1000.

3.3.3 Sensitivity to *c* and *β*

Figure 3.9 shows the sensitivity of *E* to *β* for *c* varying between 100 and 3000 m, with *a* = 2 m and *b* = 50 m. When *c* is equal to or larger than 1500 m, as shown, the differences of *E* among different cases are considerably small, i.e., the length effect is negligible. For *c* = 500 and 1000 m, the length effect is negligible for a large range of *β*, but remarkable for *β* larger than 700, resulting in a smaller and larger *E* respectively, and the failure of the linear relationship between *E* and *β*. For *c* = 100 m, the length effect is significant and the impact of *β* on *E* is highly weakened.

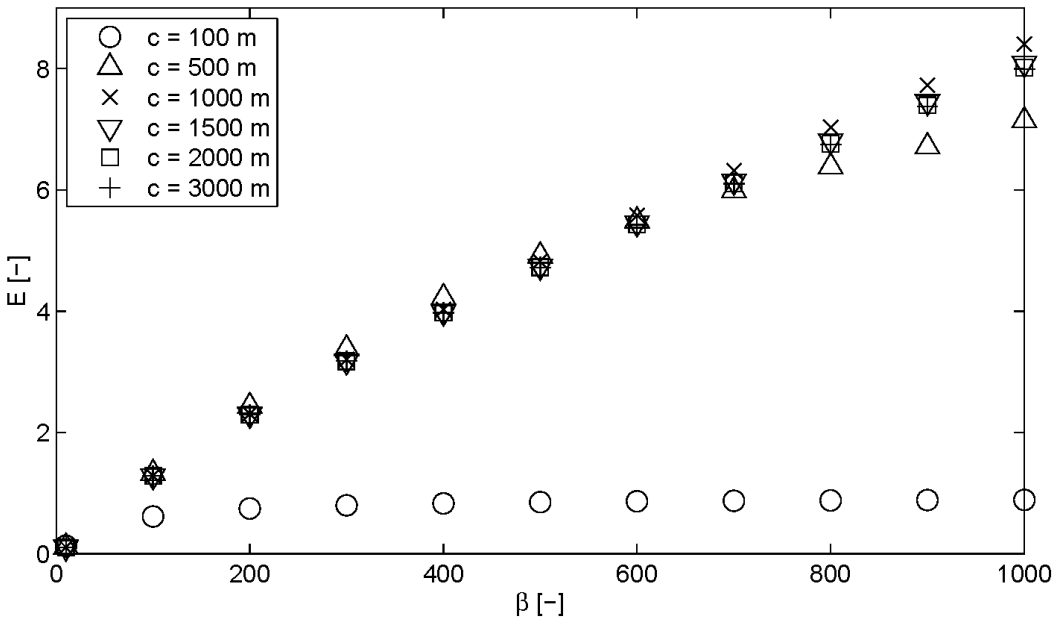

Figure 3.9. Sensitivity of *E* to *β* for *c* varying between 100 and 3000 m, in which *a* = 2m and *b* = 50 m.

Chapter 4

UNDERSTANDING THE PUMPING EFFICIENCY UNDER THREATS OF SALINE WATER UPCONING IN HETEROGENEOUS POROUS MEDIA

In a real situation, complex geological conditions result in spatial heterogeneities of aquifers' permeability at different scales. Stochastic analysis is an effective method to achieve the mean behavior of the saltwater up-coning process in a randomly distributed permeability field. Such a method has been adopted in a number of studies exploring SWI [e.g., 43, 67]. For example, Kerrou and Renard [68] applied a stochastic study to examine the impact of heterogeneity on the extent of SWI. They found that the SWI extent presented opposite behaviors in a two-dimensional model to that in a three-dimensional one. Specifically, as the degree of heterogeneity increased, the SWI extent moved seaward in 2D models, while it moved landward in 3D models. However, a limitation of their research was the use of a single realization. In a recent study by Pool et al. [69], the combined effects of spatial heterogeneity and tidal fluctuations on the SWI process in a three-dimensional aquifer were investigated. The authors verified the conclusions of Kerrou and Renard through applying more Monte Carlo simulations. Additionally, they found that the mixing phenomenon is linearly dependent on the arithmetic mean of correlations lengths in the three directions, and the variance of permeability fields.

In the present chapter, the aim is to quantitatively and qualitatively evaluate the impact of spatial variations of permeability on the SU process. An axisymmetric density-dependent flow in an anisotropic medium were simulated numerically. The primary aim is to explore how the random hydraulic conductivity fields impact the pumping efficiency. This research extends the study of

heterogeneity's impact on SU through adopting more realistic settings, and it could provide significant implications for understanding the SU process in a heterogeneous aquifer with randomly distributed permeability field.

4.1 Method

Figure 4.1 presents the conceptual model applied in this research, which is also based on the study by Zhou et al. [8] as in the previous chapter. However, the distinguished feature of the conceptual model here is the random *k* fields inserted in the model domain instead of the low-*k* layer. All conditions within the domain described in the previous chapter, such as boundary conditions were also used in this chapter, except that the discretization method and hydraulic conductivities adopted are varied. For all cases in this chapter, the domain is discretized into 75 layers and 307 columns, the same degree of discretization as in the homogeneous case. For hydraulic conductivities, values are varied across the domain, and are characterized by a random spatial function

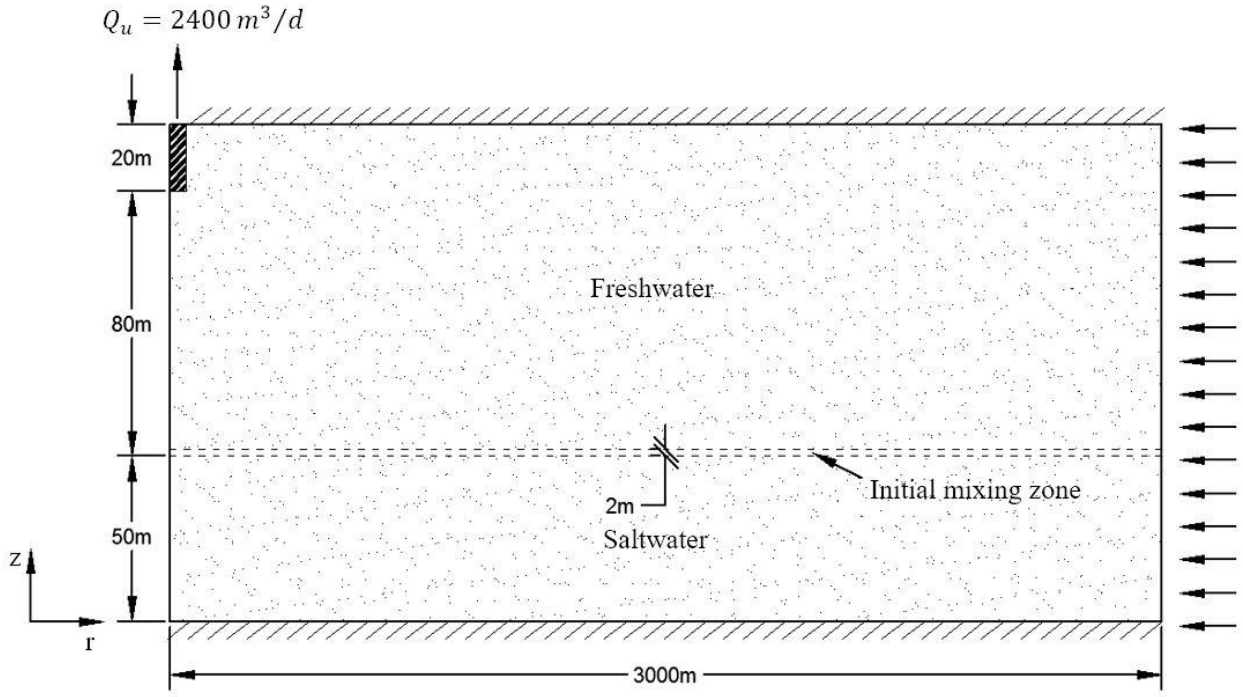

Figure 4.1. Conceptual model of a saltwater upconing in an aquifer with random distributions of hydraulic conductivity fields

Three pertinent variables for generating a random distribution of a hydraulic conductivity (*K*) field are: (I) geometric mean (μ), (II) variance (σ^2), (III) statistical anisotropy that is defined by the ratio of the vertical correlation length of the log *K* field (λ_z) to the horizontal one (λ_r). The *K* fields adopted follow a Gaussian distribution. When determining appropriate correlation lengths, the domain size and mesh size should be considered. The model domain is a 2D rectangular with an extent of $L_r \times L_z$, which is meshed into grid cells of size $d_r \times d_z$. To ensure the consistence of statistical properties of all realizations, the sizes are expected to satisfy that $d_r \ll \lambda_r \ll L_r$ (the same condition applies for the vertical direction), but that also needs to compromise the computational effort. Two series were examined in terms of varying the geometric mean and variance of *K* fields, and Table 4.1 lists the variables used for the generation of random fields. The

values used are based on the study by Prasad and Simmons [70], who also used the Monte Carlo simulations to examine the unsteady density driven flow where a dense fluid is overlying a lighter one. The case with $k_x = 2.56\times10^{-11}$ m^2, $k_z = 1.0\times10^{-11}$ m^2, and $\sigma^2 = 0.16$ served as the reference case, and the level of heterogeneity is varied by changing the values of variance. For each set of variables, 60 scenarios of specified patterns of hydraulic conductivity were obtained. These random *K* fields were then converted to account for the cylindrical coordinates in Equations 3.1.

Table 4.1. Input parameters for stochastic random *K* fields

Parameter	**Symbol**	**Value**	**Unit**
Geometric mean of permeability in the horizontal direction	k_x	2.56×10^{-10} 2.56×10^{-11} 2.56×10^{-12}	m^2
Geometric mean of permeability in the vertical direction	k_z	1.0×10^{-10} 1.0×10^{-11} 1.0×10^{-12}	m^2
Variance	σ^2	0.04, 0.16, 0.36	
Correlation length in the horizontal direction	λ_x	200	m
Correlation length in the vertical direction	λ_z	30	m

4.2 Result and discussion

4.2.1 K fields distribution

Some typical random *K* fields used in the simulations are presented in Figure 4.2 and 4.3. The red color represents the zone with relatively high *K* values, while the blue color represents the low *K* values. The *K* values in the vertical direction were assumed much smaller than those in the horizontal direction, as a common situation in real geological settings. Figure 4.2 presents random

K fields for different levels of heterogeneity. For relatively low degrees of heterogeneity, *K* fields are quite uniform and very similar to the homogeneous case, while, increasing the variance, high *K* values (e.g. almost 125 m/d) occurred in the realization (Figure 4.2e). In real geological conditions, the hydraulic conductivity value can experience large variations depending on the aquifer material. High *K* value obtained in this case might represent materials with pervious property, such as well-sorted gravel. It is assumed that flow and solute will migrate fast in these regions. Figure 4.3 presents three realizations generated from the exactly same input variables (i.e. the same geometric mean, variance, and correlation lengths), but with significantly different pumping durations (i.e. the scenario with the longest pumping duration, the very similar pumping duration to the homogeneous case, and the shortest pumping duration).

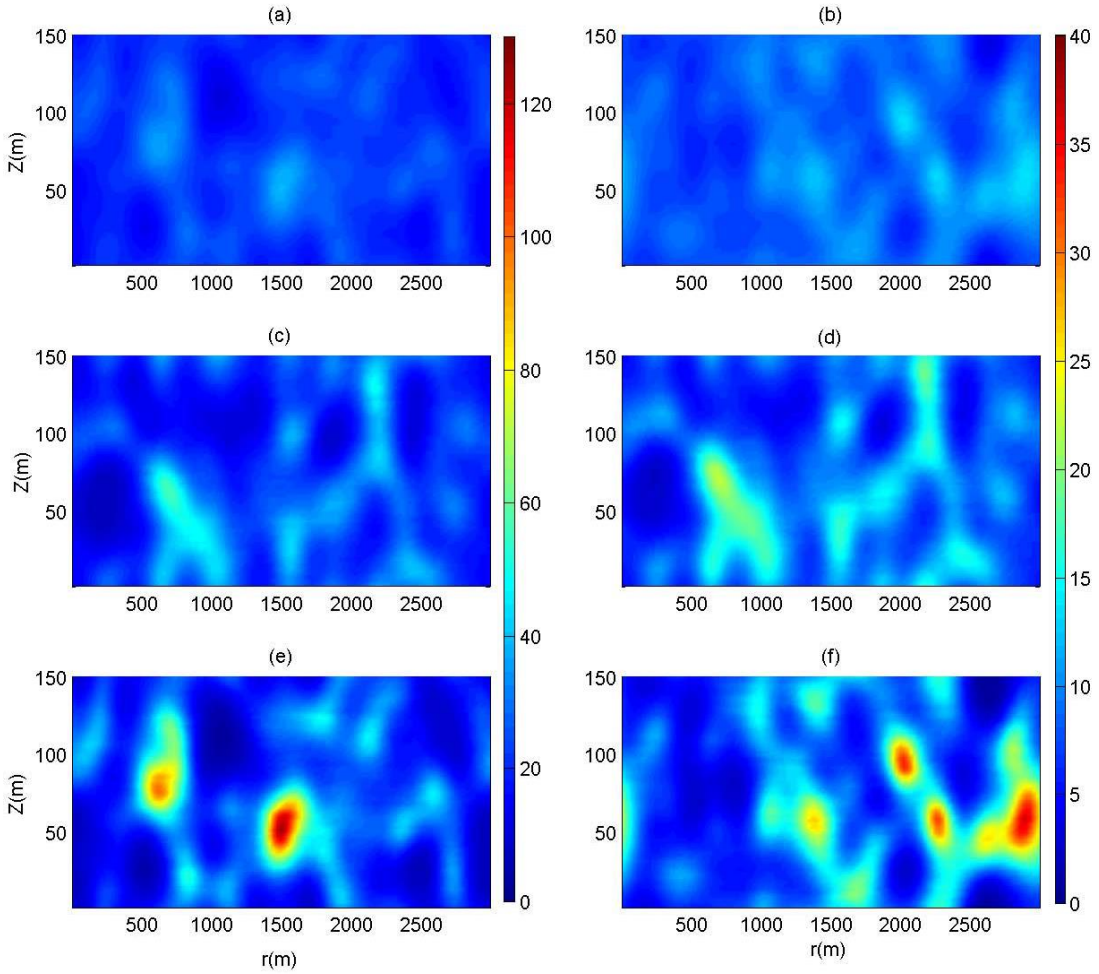

Figure 4.2. Three random K realizations generated with different variances: from the top to the bottom are 0.04, 0.16, and 0.36. The left panel shows K_r and the right panel shows K_z.

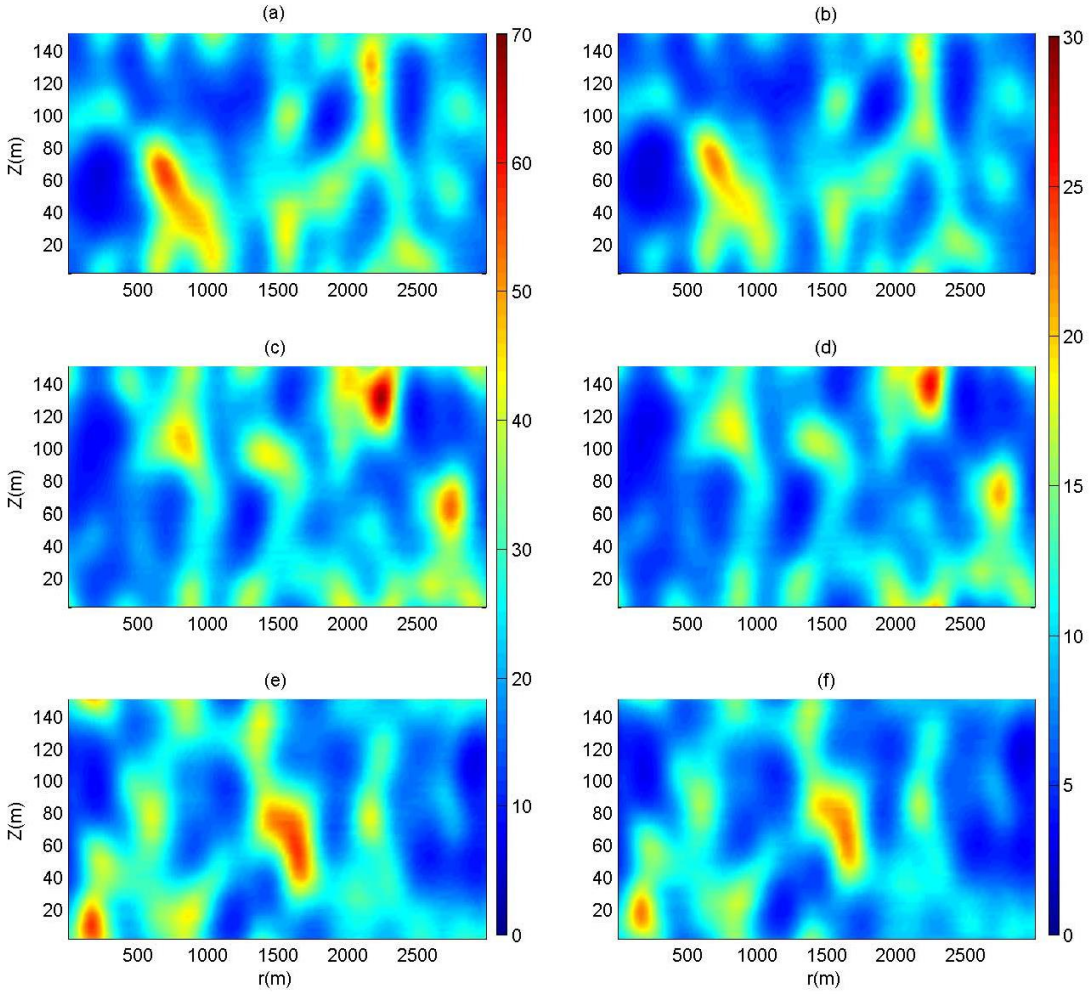

Figure 4.3. Three random *K* realizations with special pumping durations: from the top to the bottom are the realization with minimum pumping duration, similar pumping duration to homogeneous case, and the maximum pumping duration. The left panel shows K_r and the right panel shows K_z.

4.2.2 Impact on the breakthrough curves of water salinity

Available pumping durations of 60 Monte Carlo simulations for the reference case were presented through a boxplot in Figure 4.4. The pumping durations for these 60 random *K* fields show a wide range, extending from the shortest duration of about 900 days to the longest time of nearly 6600 days, with the median time of 2207.5 days suggesting that most of random realizations

are with longer pumping durations than that of the homogeneous case. Figure 4.5 presents the breakthrough curves for those featured values (i.e. the minimum, median and maximum pumping durations whose corresponding random *K* fields refer to those in Figure 4.3). Although the end pumping durations show significantly wide ranges, the times when the well started to pump salts are quite close among them (this is indicated by the fact that the intercepts are similar), and it did not take long time to pump salts (in some realizations, the results show that pumped water was contaminated by salts at the beginning of pumping, and thus no freshwater was pumped). Therefore, the long pumping duration obtained in the result (the green line) is mainly achieved due to the low rate of pumping salts, indicated by the mild slope of the curve. This pattern of extension of pumping duration is different from that in an aquifer with low-*k* layer. In the previous section, most breakthrough curves showed a long time for non-salt-pumped period (refer to Figure 3.4), thus leading to an extended available pumping duration, which is expected as the low-*k* layer performs as a hydraulic barrier to prevent the transport of salts. The mechanism responsible for the obtained breakthrough curve for randomly heterogeneous systems are qualitatively discussed in the section 4.2.5.

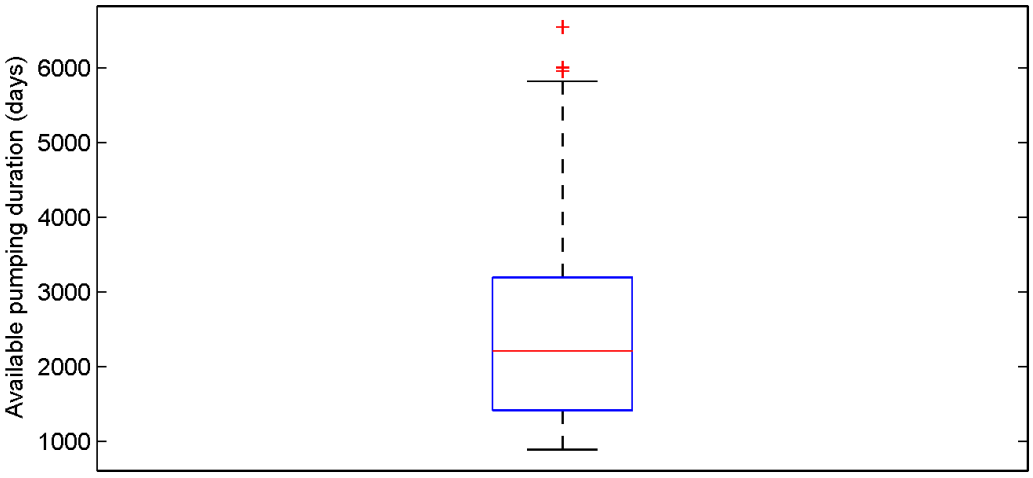

Figure 4.4. Pumping durations for 60 realizations with the same input variables

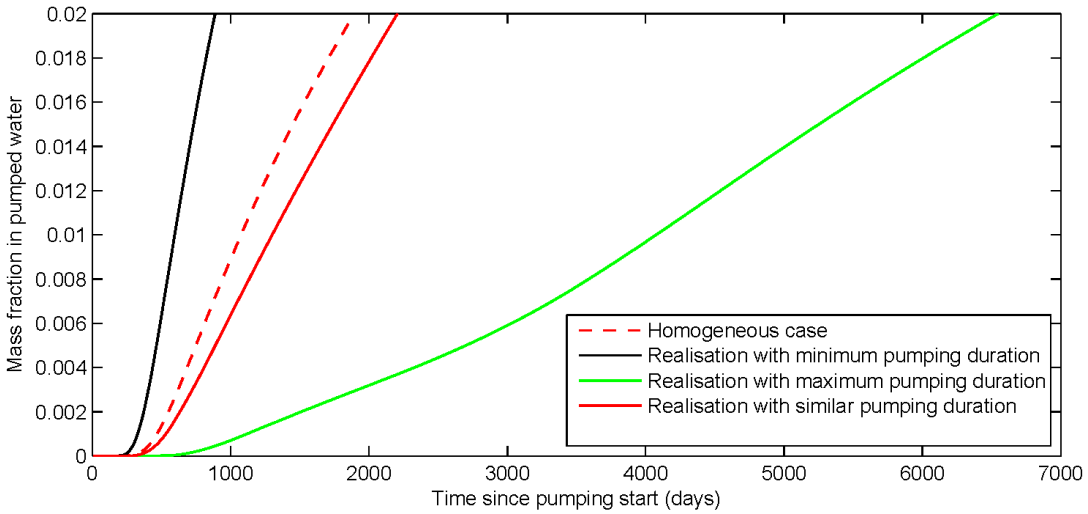

Figure 4.5. Breakthrough curves for the homogeneous case (the red dotted line) and the realizations shown in Figure 4.3.

4.2.3 Impact on salinity distribution within domain

Figure 4.6 compares transient salinity distributions corresponding to pumping in the homogeneous case and the realization with maximum pumping duration shown in Figure 4.3. The model domain with random distributions of high *K* values and low *K* values is supposed to exhibit a significantly irregular concentration profile, because the flow and solute transport are expected to choose the preferential paths to be discharged. However, the concentration profiles obtained do not vary significantly as a whole. It still shows a somehow typical upconing concentration profile, which means that two distinguished upconing regime can be recognized [8]: the upconing region (0 m < r < 500 m) is with thick salt plume induced by the above extraction well, and the region (r > 500 m) further away from the upconing region is with relatively horizontal and thin zone of salts. This may be because the high extraction rate adopted in this study leads to a very large vertical hydraulic gradient. Despite that, some fluctuations of the contour line owing to random distributions of hydraulic conductivities within the model domain can still be noticed. For example, the fluctuation of 0.02 isochor in Figure 4.6f is especially obvious in the junction between the high-*K* and low-*K* regions (refer to Figure 4.3f)

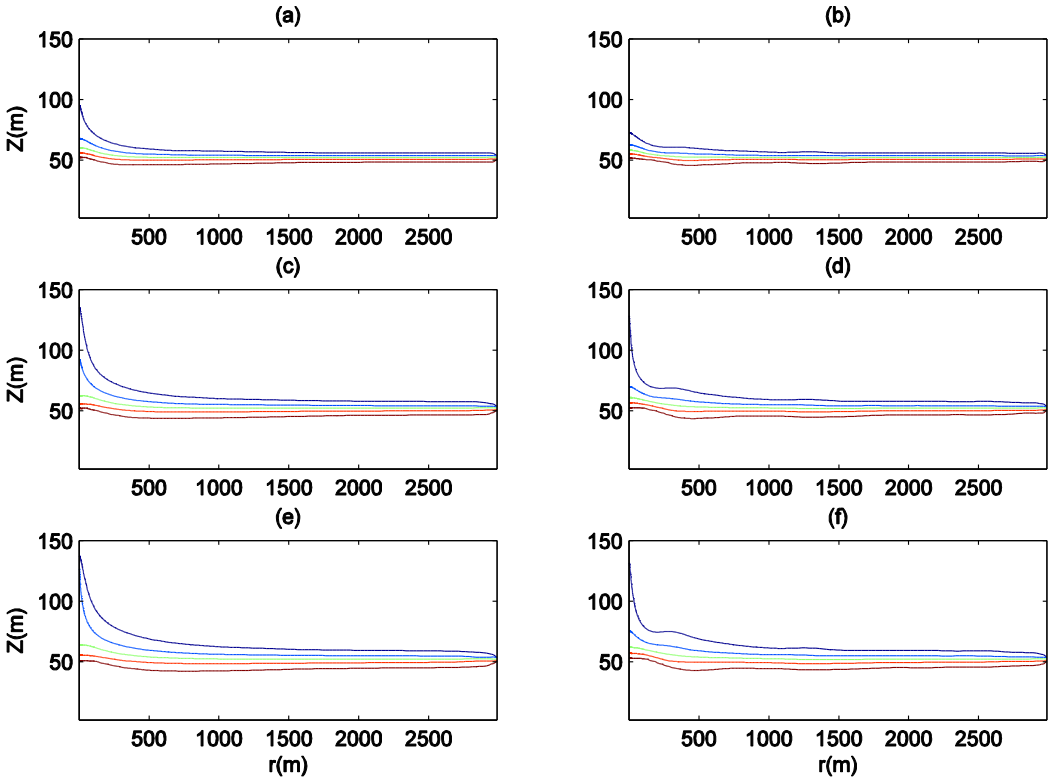

Figure 4.6. Transient salinity distributions for the homogeneous case (the left panel) and the realization with maximum pumping duration presented in Figure 4.3 (the right panel). From the top to the bottom are results after 1 year-pumping, 3-year pumping, and 5-year pumping. In each salinity distribution profile, from the top isochor to the bottom one are 0.02, 0.2, 0.5, 0.8 and 0.98.

4.2.4 Impact of level of heterogeneity

The degree of heterogeneity is a key parameter of interest when describing a heterogeneous aquifer. The focus of its impact on upconing of saltwater due to a pumping well is the available pumping duration in this section. Figure 4.7 presents three boxplots summarizing the pumping durations of 60 realizations for three systems with varied variances. Increasing the degree of heterogeneity leads to a larger variance of pumping durations, as expected. More specifically, such an impact is more obvious on the side of extending the pumping duration, which is supported by

the fact that the upper tail is lengthened to a larger extent than the lower one. Moreover, the median value is further upward away from the black dotted line (the pumping duration for the homogeneous case). These results imply that in an aquifer with a higher level of heterogeneity, the pumping duration is more likely to be extended. The Kruskal-Wallis test was used to examine the relationship among the pumping durations for these three systems. Kruskal-Wallis test is a statistical non-parametric test for three or more groups of data. The null hypothesis is that the data in each group comes from the same distribution. The alternative hypothesis is that not all samples come from the same distribution. The returned *p* value of 0.4572 indicates that Kruskal-Wallis accepts the null hypothesis at a 1% significance level.

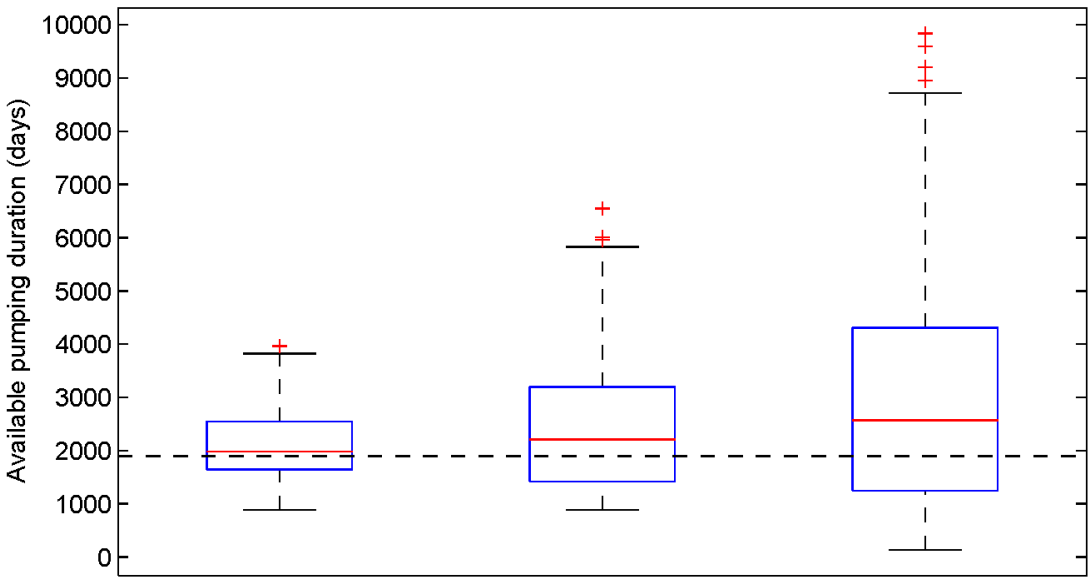

Figure 4.7. Pumping durations of 60 realizations for three varied variances: from the left to the right are 0.04, 0.16, and 0.36 (the black dotted line is the result for the homogeneous case)

4.2.5 Impact of geometric mean value

The geometric mean was also varied to a larger and smaller values (refer to Table 4.1) to test whether SU showed sensitivity to it. Intuitively, the K value is positively related to the movement of fluid flow and solute transport. That is to say increasing K value is expected to shorten the pumping duration, and vice versa. However, simulation results showed an opposite phenomenon. Specifically, for scenarios with magnitudes of both K_r and K_z (the geometric mean of K fields) decreased by 10 times, among the 60 realizations simulated, the maximum value obtained was only 1360 days. On the other hand, when they were both increased by 10 times, within the simulation time (20000 days), it failed to reach the 2% salinity. The boxplots of pumping durations for the media with different geometric means are presented in Figure 4.8 (the pumping durations for random fields with the geometric mean one magnitude larger were not obtained due to the computational effort).

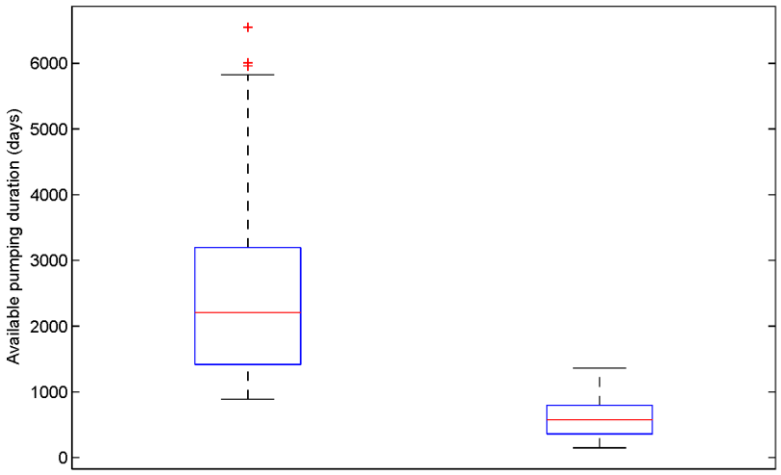

Figure 4.8. Pumping durations of 60 realizations for the case with the geometric mean equaling to the K value of homogeneous case (the left panel), and the case with the geometric mean one magnitude less than that of homogeneous case (the right panel).

Actually, De Louw et al. [39], who studied a natural process of SU in the Dutch Deep Polders through field investigations indicates a similar pattern in their study: horizontal *K* shows a negative relation to the boil salinity, while vertical *K* shows little impact on it (refer to Figure 8 [39]). This can be explained by the fact that, after increasing horizontal *K*, the lower part of saltwater zone is almost stable and only the upper part with very low salt concentrations contributes to the boil salinity (refer to Figure 7e [39]). A similar result was also obtained in this research. Figure 4.9 presents the salinity distributions within the model domain for two varied geometric means. It shows that when the magnitude of geometric mean of *K* fields was increased, only the 2% isochor was disturbed by the pumping, but the high concentration isochor were nearly horizontal. So the salinity of pumped water could hardly reach 2% even after a long-period pumping. On the contrary, in a medium with lower geometric means, all the isochor moved upwards to the well, so that the pumped water reached 2% salinity only after 584 days.

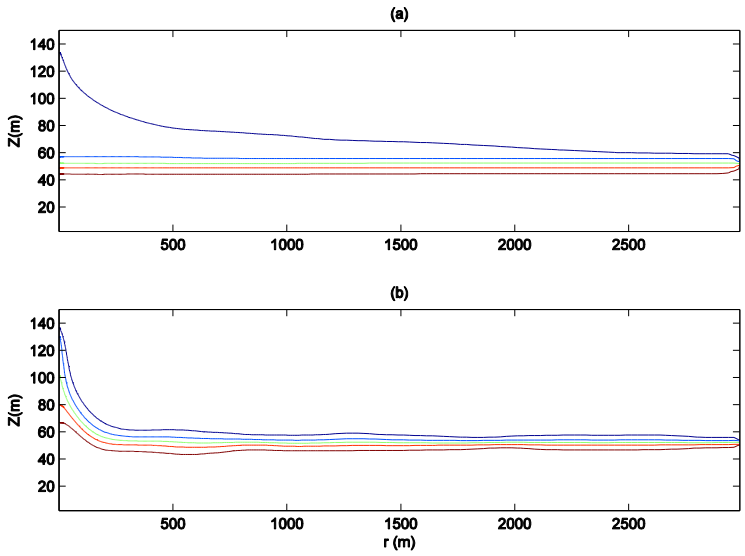

Figure 4.9. Salinity distributions for two scenarios: (a) with geometric mean of *K* fields one magnitude larger after 20000-day pumping; (b) with geometric mean of *K* fields one magnitude smaller at the time of well's shut-off. From the top to the bottom, isochor are 0.02, 0.2, 0.5, 0.8, and 0.98.

To examine whether K_r or K_z is dominant for the above results, two more scenarios were simulated. In addition to a specific realization with both geometric means of K in two directions were increased (the same realization in Figure 4.9a), scenario with only K in one direction increased for each time was included. Figure 4.10 and 4.11 shows their simulation results in terms of concentration profiles and breakthrough curves after 10000-day of continuous pumping, respectively. Firstly, the three concentration profiles show that, in two scenarios with increased horizontal K values (Figure 4.10a and 4.10b), both profiles exhibited the above described phenomenon, i.e., results that only low-concentration isochor moved upward, so that they both failed to reach the 2% water salinity during the pumping period. On the contrary, in the concentration profile with a relatively small K_r value (Figure 4.10c), even the high-concentration isochor at the bottom of the saltwater zone was disturbed, and thus the pumped water was much quicker to get a high concentration. The specific salinity within the three wells after 10000-day pumping was also calculated and presented in Figure 4.11. The significantly higher water salinity for the scenario with smaller horizontal K is identical to its concentration profile. The salinities of Figure 4.11a and 4.11b suggest that although their concentration profiles show very similar behaviors, the larger vertical K did increase the water salinity, but to a limited level compared with the effect of horizontal K. Moreover, the breakthrough curves show another pattern of impact regarding to the non-saline-water pumped period. Specifically, two scenarios with larger vertical K exhibits relatively short periods for just pure freshwater pumped, while that period for the scenario with small K_z value is almost 3500 days later.

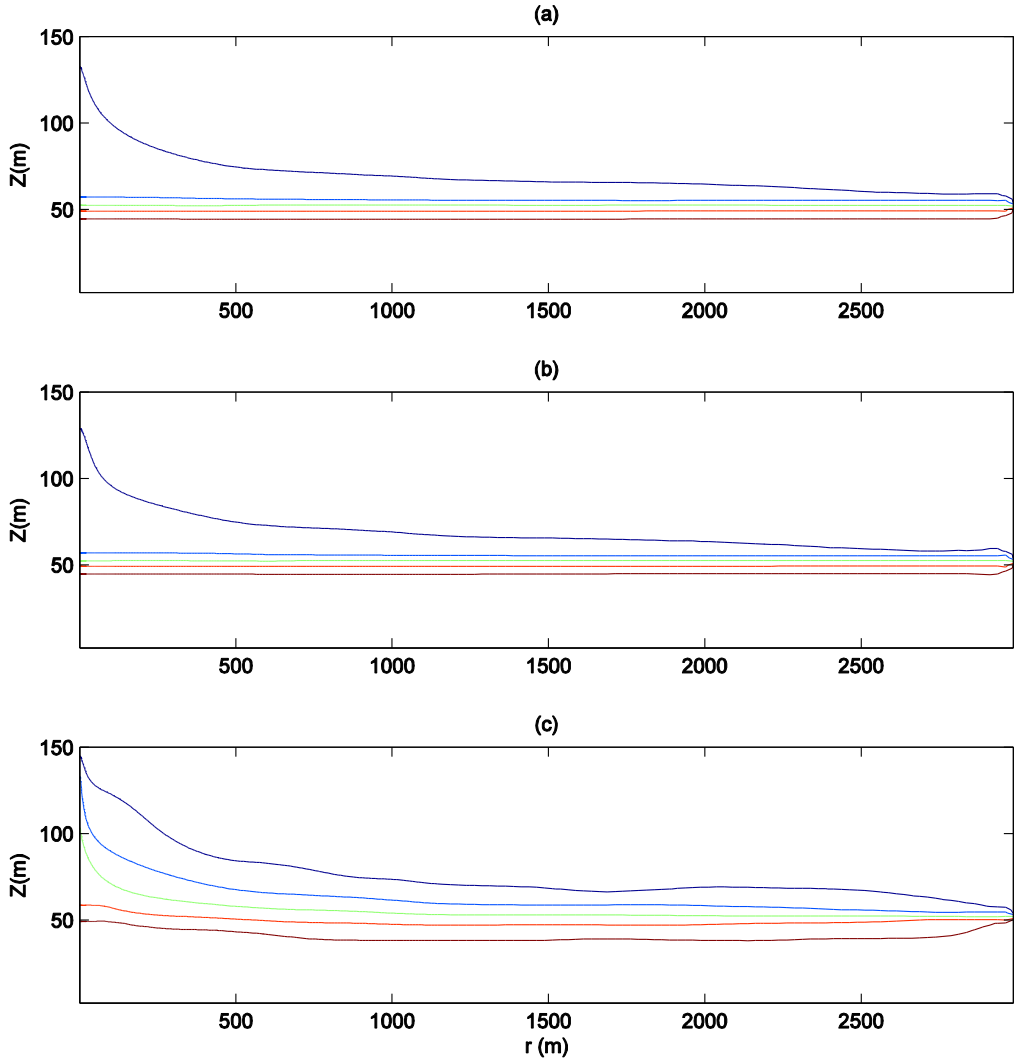

Figure 4.10. Salinity distributions after 10000-day pumping for (a) realization with increased K_r and increased K_z (the same realization with Figure 9a); (b) realization with increased K_r but original K_z (based on K values of homogeneous case); (c) realization with original K_r but increased K_z. From the top to the bottom, isochor are 0.02, 0.2, 0.5, 0.8, and 0.98.

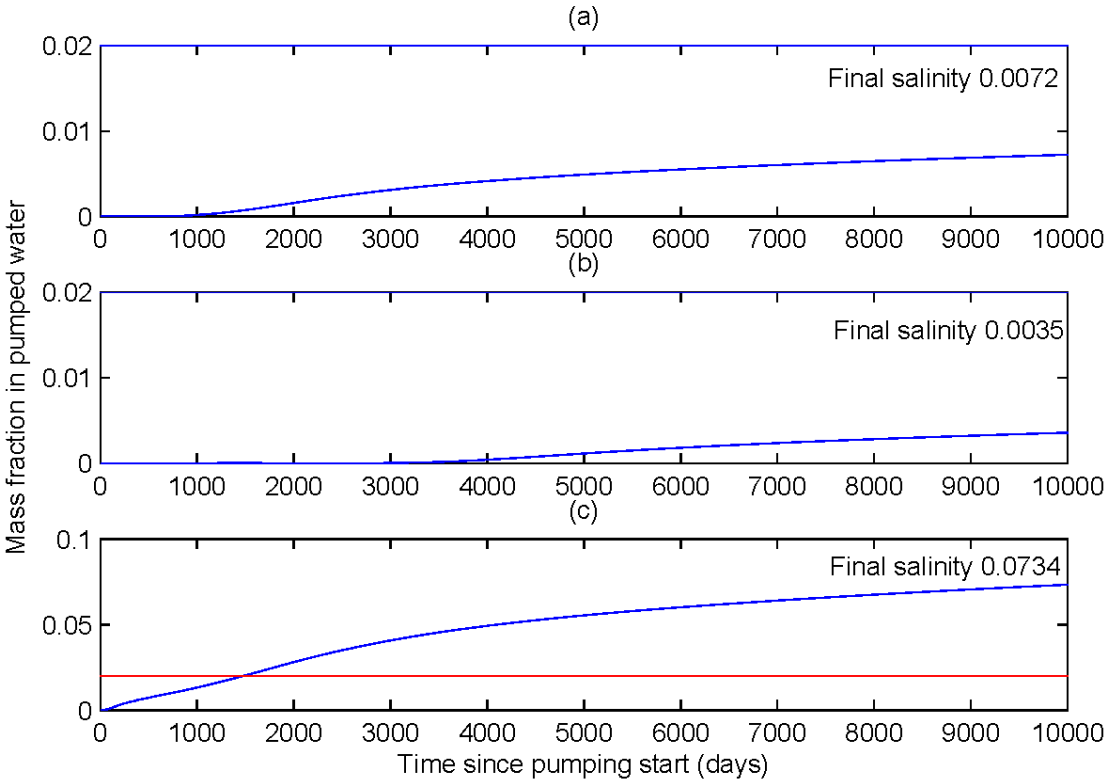

Figure 4.11. Breakthrough curves for scenarios corresponding to the Figure 4.10. The red straight line represents the threshold value for drinking purpose.

Overall, the above results suggest that *K* values in two directions show different patterns of impacts on SU induced by an extraction well. The horizontal *K* is the dominant factor for the SU process because it determines the regions of saltwater zone that contribute to the water salinity, and thus impacts both the pumping durations and concentration profiles. The vertical *K* shows limited impact on the final pumping durations; however, it can impact the early stage of pumping by affecting the time when just pure freshwater can be pumped.

However, for realizations with the same geometric mean, varied pumping durations were also obtained. For example, Figure 4.5 presents the varied breakthrough curves for realizations

shown in Figure 4.3 with the same geometric mean in two directions. It can be noticed that, for the scenario with the similar pumping duration to the homogeneous case (Figure 4.3c and 4.3d), its realizations show that, within the regions from the well-side boundary to nearly 500 m away, the *K* values in two directions are similar to that of homogeneous one (i.e. K_r = 21.6982 m/d and K_z = 8.4758 m/d). As for the scenario with the shortest pumping duration (Figure 4.3a and 4.3b), within the same region, the *K* values are observed to be smaller than those of homogeneous case. As for the scenario with the maximum pumping duration (Figure 4.3e and 4.3f), relatively larger *K* values in two directions are noticed within the region. Referring to the concentration profiles (see Figure 4.6), such a region (0 m < r < 500 m) just describes the upconing region defined in the previous section. Furthermore, when considering the non-saline-water pumped period in the breakthrough curves (see Figure 4.5), a distinguished time frame from the other three values was noticed for the scenario with the maximum pumping duration. Such a result is consistent with the pattern that its K_z values presented within the upconing regions (Figure 4.3f). That means, the only high *K* zones exhibited within the upconing region caused the longer time to start to pump salts. The above results described for the same geometric mean are identical to those obtained for different geometric means. So it is summarized that the pattern how hydraulic conductivities impact SU is highly related to their values within the upconing region, which might be described as effective *K* values in terms of affecting SU process. However, this should be further studied by testing more scenarios.

Chapter 5

CONCLUSIONS, IMPLICATIONS AND LIMITATIONS

5.1 Conclusions and implications

5.1.1 Layered aquifer

Chapter 3 included the numerical simulation results for modelling SU occurring in an aquifer with an aquitard, which was implemented by inserting a horizontal low-*k* layer in a homogeneous aquifer. Detailed discussions of the impact of an aquitard on SU was provided in the chapter, among which two main conclusions can be withdrawn as follows:

1. The low-*k* layer could alter significantly the flow patterns and thus reduce or impede SU. A sound linear relationship can be found between β (Equation 3.4) and E (Equation 3.3), if the radius of the low-*k* layer is large enough. A thicker low-*k* layer leads to a larger E under otherwise the same conditions.
2. There exists a critical location of a low-*k* layer where the well is allowed to pump for a longest period (i.e. the maximum E). This critical location is below and near the bottom of the well. When the low-*k* layer penetrates the well, E decreases sharply with decreasing b (Figure 3.1). When the low-*k* layer is located below this critical location, by contrast, E decreases relatively gently with increasing b.

Despite the model being highly simplified and neglecting many other factors such as regional flows and unsteady pumping conditions, the results developed could provide significant implication for improving pumping efficiency under the threats of saltwater upconing through natural and artificial barriers. Specifically, when there is an aquitard in the subsurface, it is

suggested that the partially penetrating well does not reach this natural barrier. Otherwise, the efficiency of the well could be significantly lowered. On the other hand, one could develop an artificial barrier below the well bottom to improve pumping efficiency. The obtained linear relationship between β and E together with the understanding of the effects of a, b, and c on E could assist in the design of an effective artificial barrier.

5.1.2 Randomly distributed aquifer

Numerical simulation results of SU in randomly distributed hydraulic conductivity fields, representing the random heterogeneity in real situations, were included in Chapter 4. There are also two primary conclusions summarized from simulation results:

1. Pumping efficiency of wells located in randomly heterogeneous aquifers may behave with large variances, and these variances of behaviors would be more obvious in aquifers with higher degrees of heterogeneity, which poses difficulties to predict SU in such aquifers. Despite that, pumping efficiency of a well in aquifers with higher degrees of heterogeneity might be more likely to be improved, compared with that in aquifers with lower degrees of heterogeneity. This is indicated by the result that the higher degrees of heterogeneity is, the larger portion of realizations show longer pumping durations than that of homogeneous case.
2. For anisotropic aquifers, vertical and horizontal values of hydraulic conductivities show different patterns of impact on pumping efficiency. Vertical ones are more associated with the non-pumping-salt period, while horizontal ones are dominant for the end pumping duration. Specifically, the larger the vertical hydraulic conductivity is, the shorter non-pumping-salt period will be. On the contrary, the larger the horizontal hydraulic conductivity is, the longer end pumping duration will be, which is because the salt

contributing region is only from the upper low-isochor zone. Vertical and horizontal hydraulic conductivities within the upconing region (i.e. the region where upward movements of isochor are obvious) are dominant for these patterns of impacts than those in the far away region.

The conclusions obtained can have important implications for understanding pumping in a randomly heterogeneous aquifer under threats of saltwater upconing. If the permeability of an aquifer is randomly distributed with large variances of permeability values, that is to say the degrees of heterogeneity is high, the efficiency of the pumping well located in such an aquifer is more likely to be improved. Also, when there are relatively permeable materials presented, such as gravels or well-sorted sands horizontally connected in the aquifer, especially within the regions that close to the pumping well, the efficiency of the pumping well could be significantly improved. So if the location of an extraction well is selected considering the above suggestions, using a natural geological condition in an aquifer instead of any artificial technologies may be capable to increase the pumping efficiency.

5.2 Limitations

This work is an elementary study of SU in fields with heterogeneity in terms of hydraulic conductivities, which was not investigated in published works. The limitations of the current research are summarized as the following:

1. This study was purely numerical and applied to the idealized scenario of Zhou et al. [8]. For future work, it is suggested to include physical experimental work or

calibration of numerical models with field data to validate the results in the current study.

2. A very simple and perfect layer was used for representing a stratified aquifer. However, in a realistic field condition, stratified aquifers can be much more complicated. This can be extended by testing SU in multilayered aquifers with varied ranges of hydraulic conductivities.
3. The conclusions obtained from current study, such as the critical location, may be not valid for other cases, because specific dimensional parameters were adopted in this research. This can be further studied by simulating more cases with different settings, and then find their dimensionless relationships.
4. For random heterogeneity, the sensitivity of pumping durations to the statistical property of correlation lengths was not examined.
5. The current study is limited to local upconing, so that regional flow was not considered here. The field of SU in heterogeneous aquifers with regional flows is lack of understanding, and this may be studied in future researches.
6. The detailed study of effective values of hydraulic conductivities regarding to their impacts on pumping durations was required for better understanding. For example, this could be achieved by examining scenarios with high geometric mean for entire domain but small values within the upconing region.

References

1. *Groundwater Quality* Available from: http://www.ga.gov.au/scientific-topics/water/groundwater/understanding-groundwater-resources/groundwater-quality.
2. Bear, J. and Q. Zhou, *Sea water intrusion into coastal aquifers*, in *The handbook of groundwater engineering* J.W. Delleur, Editor. 2006.
3. Bear, J., *Sea Water Intrusion into Coastal Aquifers*, in *Encyclopedia of Hydrological Sciences*. 2006, John Wiley & Sons, Ltd.
4. Xue, Y., et al., *Sea-Water Intrusion in the Coastal Area of Laizhou Bay, China: 1. Distribution of Sea-Water Intrusion and Its Hydrochemical Characteristics.* Ground Water, 1993. **31**(4): p. 532-537.
5. Mustafa S, S.S., Barnett S, *Preliminary Investigation of Seawater Inrusion Into a Fresh Water Coatsal Aquifer - Lower South East, DEWNR Technical Report 2012/01*, W.a.N.R. Government of South Australia through Environment, Editor. 2012.
6. Werner, A.D., et al., *Seawater intrusion processes, investigation and management: recent advances and future challenges.* Advances in Water Resources, 2013. **51**: p. 3-26.
7. Simmons, C.T., T.R. Fenstemaker, and J.M. Sharp Jr, *Variable-density groundwater flow and solute transport in heterogeneous porous media: approaches, resolutions and future challenges.* Journal of Contaminant Hydrology, 2001. **52**(1–4): p. 245-275.
8. Zhou, Q., J. Bear, and J. Bensabat, *Saltwater Upconing and Decay Beneath a Well Pumping Above an Interface Zone.* Transport in Porous Media, 2005. **61**(3): p. 337-363.
9. Langevin, C.D., *Modeling axisymmetric flow and transport.* Groundwater, 2008. **46**(4): p. 579-590.
10. Bear, J., et al., *Seawater intrusion in coastal aquifers: concepts, methods and practices*. Vol. 14. 1999: Springer Science & Business Media.
11. Reilly, T.E. and A.S. Goodman, *Quantitative analysis of saltwater-freshwater relationships in groundwater systems—A historical perspective.* Journal of Hydrology, 1985. **80**(1): p. 125-160.
12. Reilly, T.E. and A.S. Goodman, *Analysis of saltwater upconing beneath a pumping well.* Journal of Hydrology, 1987. **89**(3–4): p. 169-204.
13. Muskat, M. and R.D. Wycokoff, *An Approximate Theory of Water-coning in Oil Production.*
14. Bennett, G.D., M.J. Mundorff, and S.A. Hussain, *Electric-analog studies of Brine coning beneath freshwater wells in the Punjab region, West Pakistan*, in *Water Supply Paper*. 1968.
15. Schmork, S. and A. Mercado, *Upconing of fresh water—sea water interface below pumping wells, field study.* Water Resources Research, 1969. **5**(6): p. 1290-1311.
16. Wirojanagud, P. and R.J. Charbeneau, *Saltwater upconing in unconfined aquifers.* Journal of Hydraulic Engineering, 1985. **111**(3): p. 417-434.
17. Dagan, G. and J. Bear, *Solving the problem of local interface upconing in a coastal aquifer by the method of small perturbations.* Journal of Hydraulic Research, 1968. **6**(1): p. 15-44.
18. Motz, L.H., *Salt-Water Upconing in an Aquifer Overlain by a Leaky Confining Bed.* Ground Water, 1992. **30**(2): p. 192-198.
19. Bower, J.W., L.H. Motz, and D.W. Durden, *Analytical solution for determining the critical condition of saltwater upconing in a leaky artesian aquifer.* Journal of Hydrology, 1999. **221**(1–2): p. 43-54.
20. Barlow, P.M., *Ground Water in Fresh Water-salt Water Environments of the Atlantic*. Vol. 1262. 2003: Geological Survey (USGS).
21. Strack, O., *A single ‐potential solution for regional interface problems in coastal aquifers.* Water Resources Research, 1976. **12**(6): p. 1165-1174.

22. Garabedian, S.P., *Estimation of Salt Water Upconing Using a Steady‐State Solution for Partial Completion of a Pumped Well.* Groundwater, 2013. **51**(6): p. 927-934.
23. Hendizadeh, R., et al., *Steady critical discharge rates from vertical and horizontal wells in fresh–saline aquifers with sharp interfaces.* Hydrogeology Journal, 2016. **24**(4): p. 865-876.
24. MUSKAT, M., *The Flow of Homogeneous Fluids Through Porous Media.* Soil Science, 1938. **46**(2): p. 169.
25. Dagan, G. and D. Zeitoun, *Free‐surface flow toward a well and interface upconing in stratified aquifers of random conductivity.* Water resources research, 1998. **34**(11): p. 3191-3196.
26. Pauw, P.S., et al., *Saltwater Upconing Due to Cyclic Pumping by Horizontal Wells in Freshwater Lenses.* Groundwater, 2016. **54**(4): p. 521-531.
27. Werner, A.D., D. Jakovovic, and C.T. Simmons, *Experimental observations of saltwater up-coning.* Journal of Hydrology, 2009. **373**(1): p. 230-241.
28. Nordbotten, J.M. and M.A. Celia, *An improved analytical solution for interface upconing around a well.* Water resources research, 2006. **42**(8).
29. Bakker, M., *Transient Dupuit Interface Flow with partially penetrating features.* Water Resources Research, 1998. **34**(11): p. 2911-2918.
30. Kemblowski, M., *Salt-water—freshwater transient upconing — An implicit boundary-element solution.* Journal of Hydrology, 1985. **78**(1): p. 35-47.
31. Zhang, H., G.C. Hocking, and B. Seymour, *Critical and supercritical withdrawal from a two-layer fluid through a line sink in a partially bounded aquifer.* Advances in Water Resources, 2009. **32**(12): p. 1703-1710.
32. Guo, W. and C.D. Langevin, *User's guide to SEAWAT; a computer program for simulation of three-dimensional variable-density ground-water flow*. 2002.
33. Shalabey, M., D. Kashyap, and A. Sharma, *Numerical model of saltwater transport toward a pumping well.* Journal of Hydrologic Engineering, 2006. **11**(4): p. 306-318.
34. Jakovovic, D., et al., *Saltwater upconing zone of influence.* Advances in Water Resources, 2016. **94**: p. 75-86.
35. Voss, A. and M. Koch, *Numerical simulations of topography-induced saltwater upconing in the state of Brandenburg, Germany.* Physics and Chemistry of the Earth, Part B: Hydrology, Oceans and Atmosphere, 2001. **26**(4): p. 353-359.
36. Aliewi, A., et al., *Numerical simulation of the movement of saltwater under skimming and scavenger pumping in the Pleistocene aquifer of Gaza and Jericho areas, Palestine.* Transport in porous media, 2001. **43**(1): p. 195-212.
37. Marandi, A. and L. Vallner, *Upconing of saline water from the crystalline basement into the Cambrian--Vendian aquifer system on the Kopli Peninsula, northern Estonia/Soolaka vee ulestomme aluskorrast Kambriumi-Vendi veeladestikku Pohja-Eestis Kopli poolsaarel.* Estonian Journal of Earth Sciences, 2010. **59**: p. 277+.
38. Cai, J., T. Taute, and M. Schneider, *Saltwater Upconing Below a Pumping Well in an Inland Aquifer: a Theoretical Modeling Study on Testing Different Scenarios of Deep Saline-Groundwater Pathways.* Water, Air, & Soil Pollution, 2014. **225**(11): p. 2203.
39. De Louw, P., et al., *Natural saltwater upconing by preferential groundwater discharge through boils.* Journal of Hydrology, 2013. **490**: p. 74-87.
40. Henry, R.H., *Effects of dispersion on salt encroachment in coastal aquifers.* Geological survey water-supply paper 1613-C, 1964.
41. J, E., *Transient convection in a porous medium.* Journal of FLuid Mechanics, 1967. **27**(3): p. 609-623.
42. Larsson, A., *The international projects INTRACOIN, HYDROCOIN and INTRAVAL.* Advances in Water Resources, 1992. **15**(1): p. 85-87.

43. Held, R., S. Attinger, and W. Kinzelbach, *Homogenization and effective parameters for the Henry problem in heterogeneous formations.* Water resources research, 2005. **41**(11).
44. Abarca, E., et al., *Anisotropic dispersive Henry problem.* Advances in Water Resources, 2007. **30**(4): p. 913-926.
45. Oswald, S.E. and W. Kinzelbach, *Three-dimensional physical benchmark experiments to test variable-density flow models.* Journal of Hydrology, 2004. **290**(1–2): p. 22-42.
46. Johannsen, K., et al., *The saltpool benchmark problem – numerical simulation of saltwater upconing in a porous medium.* Advances in Water Resources, 2002. **25**(3): p. 335-348.
47. Jakovovic, D., A.D. Werner, and C.T. Simmons, *Numerical modelling of saltwater up-coning: Comparison with experimental laboratory observations.* Journal of Hydrology, 2011. **402**(3–4): p. 261-273.
48. Ma, T.S., et al., *Modeling saltwater upconing in a freshwater aquifer in south-central Kansas.* Journal of Hydrology, 1997. **201**(1): p. 120-137.
49. Aliewi, A., *Numerical simulation of the behaviour of the fresh/saline water transition zone around a scavenger well*. 1993, University of Newcastle upom Tyne, U.K.
50. List, E.J. and N.H. Brooks, *Lateral dispersion in saturated porous media.* Journal of Geophysical Research, 1967. **72**(10): p. 2531-2541.
51. Bear, J., et al., *The transition zone between fresh and salt waters in coastal aquifers*. 1960, Berkeley, CA.
52. Paster, A. and G. Dagan, *Mixing at the interface between two fluids in aquifer well upconing steady flow.* Water Resources Research, 2008. **44**(5): p. n/a-n/a.
53. Paster, A. and G. Dagan, *Mixing at the interface between fresh and salt waters in 3D steady flow with application to a pumping well in a coastal aquifer.* Advances in Water Resources, 2008. **31**(12): p. 1565-1577.
54. Pool, M. and J. Carrera, *A correction factor to account for mixing in Ghyben-Herzberg and critical pumping rate approximations of seawater intrusion in coastal aquifers.* Water Resources Research, 2011. **47**(5): p. n/a-n/a.
55. Jakovovic, D., et al., *Tracer adsorption in sand-tank experiments of saltwater up-coning.* Journal of Hydrology, 2012. **414**: p. 476-481.
56. Mehdizadeh, S.S., F. Vafaie, and H. Abolghasemi, *Assessment of sharp-interface approach for saltwater intrusion prediction in an unconfined coastal aquifer exposed to pumping.* Environmental Earth Sciences, 2015. **73**(12): p. 8345-8355.
57. de Louw, P.G.B., et al., *Upward groundwater flow in boils as the dominant mechanism of salinization in deep polders, The Netherlands.* Journal of Hydrology, 2010. **394**(3–4): p. 494-506.
58. De Louw, P.G.B., Eeman, S., Siemon, B., Voortman, B. R., Gunnink, J., van Baaren, E. S., & de Essink, G. H. P. Ou. , *Shallow rainwater lenses in deltaic areas with saline seepage.* Hydrology and Earth System Sciences, 2011.
59. García-Menéndez, O., et al., *Spatial characterization of the seawater upconing process in a coastal Mediterranean aquifer (Plana de Castellón, Spain): evolution and controls.* Environmental Earth Sciences, 2016. **75**(9): p. 728.
60. Kura, N.U., et al., *A Preliminary Appraisal of the Effect of Pumping on Seawater Intrusion and Upconing in a Small Tropical Island Using 2D Resistivity Technique.* The Scientific World Journal, 2014. **2014**: p. 796425.
61. Lu, C., et al., *Steady-state freshwater–seawater mixing zone in stratified coastal aquifers.* Journal of Hydrology, 2013. **505**: p. 24-34.
62. Liu, Y., et al., *Influence of a coarse interlayer on seawater intrusion and contaminant migration in coastal aquifers.* Hydrological Processes, 2014. **28**(20): p. 5162-5175.

63. Frind, E.O., *Seawater intrusion in continuous coastal aquifer-aquitard systems.* Advances in Water Resources, 1982. **5**(2): p. 89-97.
64. Voss, C.I. and W.R. Souza, *Variable density flow and solute transport simulation of regional aquifers containing a narrow freshwater-saltwater transition zone.* Water Resources Research, 1987. **23**(10): p. 1851-1866.
65. Verruijt, A., *Theory of groundwater flow* 1970.
66. Christian D. Langevin, W.B.S., Weixing Guo, *MODFLOW-2000, the U.S. Geological Survey Modular Ground-Water Model—Documentation of the SEAWAT- 2000 Version with the Variable-Density Flow Process (VDF) and the Integrated MT3DMS Transport Process (IMT)*. 2003, U.S. GEOLOGICAL SURVEY.
67. Abarca Cameo, E., *Seawater intrusion in complex geological environments.* 2006.
68. Kerrou, J. and P. Renard, *A numerical analysis of dimensionality and heterogeneity effects on advective dispersive seawater intrusion processes.* Hydrogeology journal, 2010. **18**(1): p. 55-72.
69. Pool, M., V.E.A. Post, and C.T. Simmons, *Effects of tidal fluctuations and spatial heterogeneity on mixing and spreading in spatially heterogeneous coastal aquifers.* Water Resources Research, 2015. **51**(3): p. 1570-1585.
70. Prasad, A. and C.T. Simmons, *Unstable density-driven flow in heterogeneous porous media: A stochastic study of the Elder [1967b] "short heater" problem.* Water Resources Research, 2003. **39**(1): p. SBH 4-1-SBH 4-21.